Africa Journal of Geosciences

Refereed scientific journal

Volume 1, 2018

ISSN: 1858-8913 (online), 1858-8905 (hard copy), http://www.iua.edu.sd

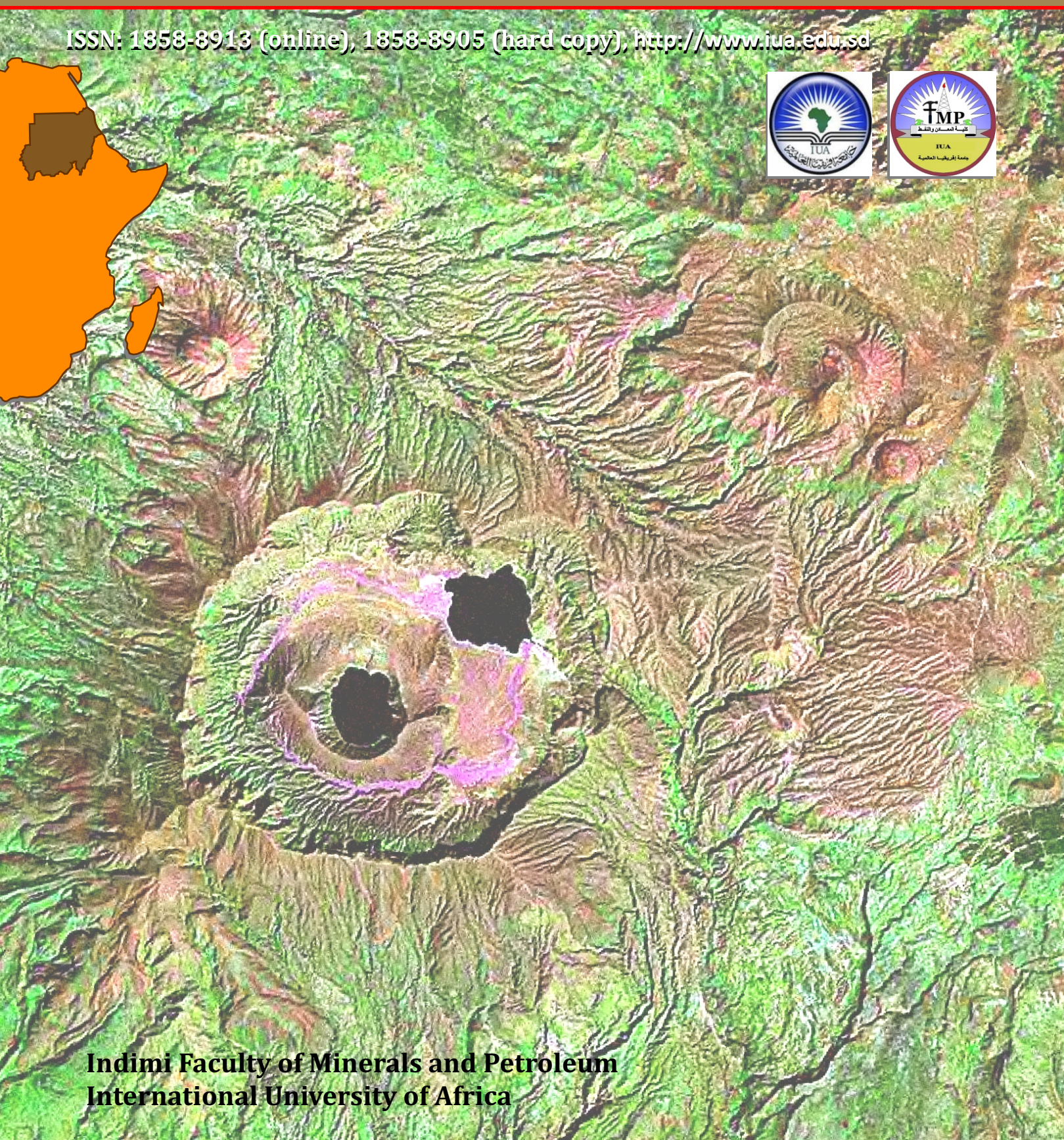

Indimi Faculty of Minerals and Petroleum
International University of Africa

مجلة افريقيا لعلوم الأرض

مجلة علمية محكمة

المجلد الأول ، ٢٠١٨

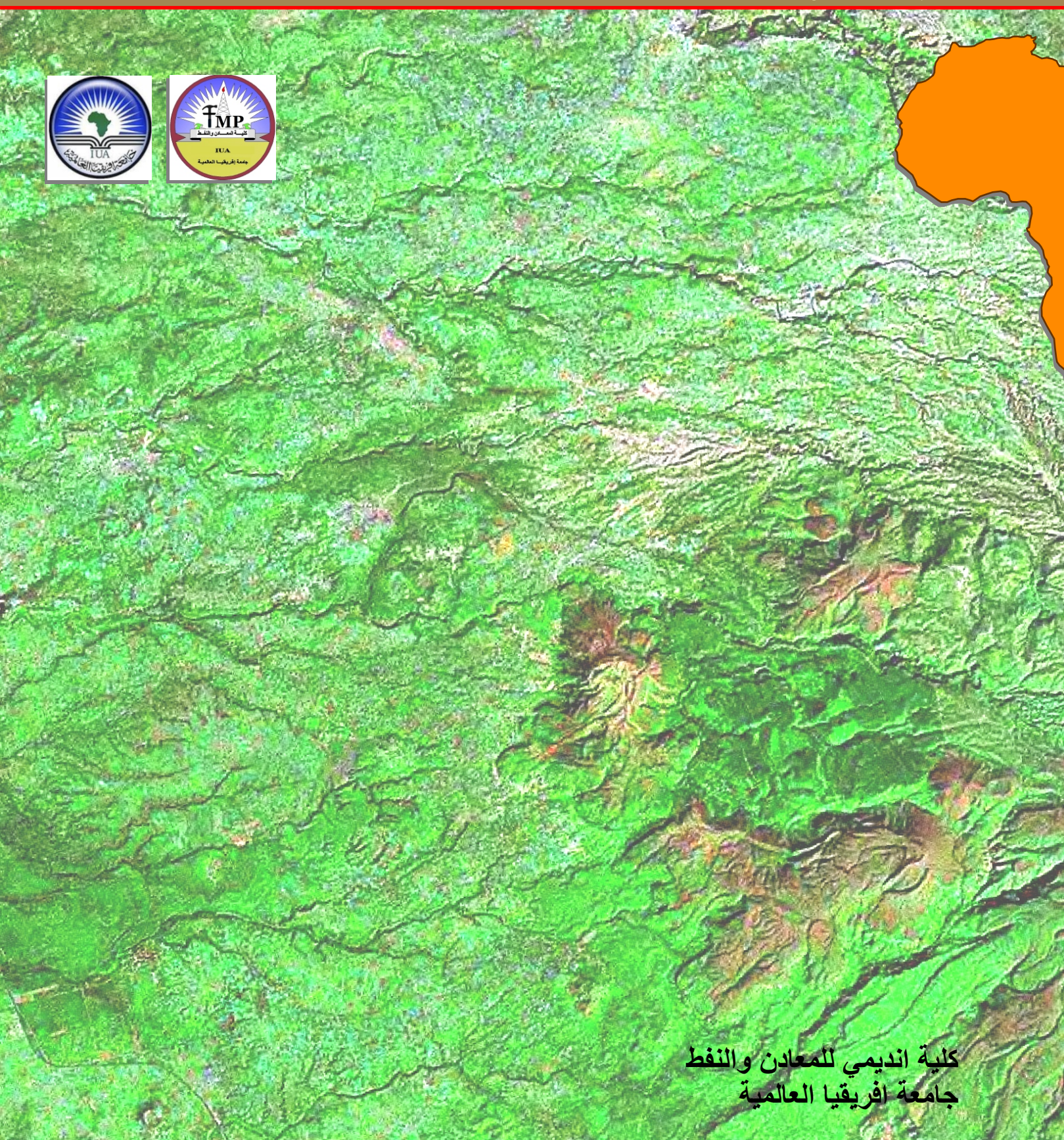

كلية انديمي للمعادن والنفط
جامعة افريقيا العالمية

Africa Journal of Geosciences (AJG)
Volume 1, 2018
ISSN: 1858-8913 (online), 1858-8905 (hard copy), http://www.iua.edu.sd

Geochemistry and Petrogenesis of the amphibolites from Jebel Kordofan - El Obeid Area, North Kordofan, Sudan.

Mustafa, H.A.*[a], Chen, N.[b,c] , Salih, M.A.[a], Abdelsamad, M.I.[a], Slama, E.M.[a,b], Wang, L.[b], Ma, C.[b] , Liao, F.[b] and Wang, L.[b]

[a] Faculty of Science, University of Kordofan, EL Obeid, P.O 160, Sudan
[b] Faculty of Earth Science, China University of Geosciences, Wuhan, 430074, China
[c] State Key Lab of Geological Processes and Mineral Resources, China University of Geosciences, 430074, China
Email: ham3019@yahoo.com

Received: 27 October 2018/ revised: 24 November 2018 / accepted: 10 December 2018

Abstract

The amphibolites from Jebel Kordofan in El Obeid area, North Kordofan in western Sudan exposed within the Precambrian Basement Complex. The precursor magmas of these amphibolites were sub-alkaline basalts derived from an arc to back arc-related tectonic setting. These amphibolites displayed LREE and LILE enrichments, strongly positive P and negative Ti anomalies, and Nb–Ta and Zr–Hf with significant spiky patterns having negative and positive Eu anomaly (Eu/Eu* = 0.89–1.03), quietly similar to E-MORB and arc-like pattern. These rocks characterized by moderate SiO_2 content from 46.7 to 50.7 wt.% suggesting typically mafic derived rocks, their very low MgO contents indicating evolved precursor magma MgO = 5.69-7.91 wt% and $Mg^{\#}$ values are 43.6–51.4. These rocks discriminated as ferrobasalts because of their high content of FeO_t between 12.3 and 13.8 wt% indicating trend of Fenner. Also they have values and ratios of $(Hf/Sm)_n$, $(Ta/La)_n$, La/Nb and La/Ta ranging between (0.92–1.09), (0.73–1.83), (0.91–2.59) and (9.20–22.8), respectively, which possibly indicated that the precursor magmas of these rocks from metasomatized sub-continental lithospheric mantle on subducted related melt environments. The study proposed that these amphibolites were probably generated in back arc environment and thus suggests a subduction tectonic regime during the Neoproterozoic period through subduction-accretion-collision.

Key words: Amphibolites, Ferrobasalts, North Kordofan, Neoproterozoic, Subduction

1. Introduction

Rodinia Supercontinent formed from continental crust that assembled during the late Mesoproterozoic and Early Neoproterozoic, through Grenvillian collisional events (late Mesoproterozoic) in span of time ~ 1100 – 750 Ma (McMenamin & McMenamin, 1990; Hoffman, 1991) taking place of time of ~ 400 m.y. Weil et al. (1998), Zhao et al. (2002) and Yoshida et al. (2003) authenticated that its final assemblage is in 1.0 Ga by the continental fragments accretion which later constitute cratonic components that form Gondwana supercontinent. Laurentia had been proposed as the core of the Rodinia supercontinent because it centered the Late Neoproterozoic passive margins which resulted during Rodinia breakup (Bond et al., 1984; Yoshida et al., 2003). The locations of Australia, Antarctica and probably South China (Li et al., 1999) represented along the western margin of Laurentia, while Baltica and Amazonia, and Rio de la Plata Craton situated along the eastern margin. Siberia lay to northern and western Laurentia's margin with uncertain position for the Congo and Kalahari Cratons (Powell et al., 2001; Yoshida et al., 2003). Rodinia reconstructions proposed that all the world's continents were gathered into a single supercontinent (Hoffman, 1991; Dalziel, 1997; Karlstrom et al., 1999; Piper, 2000; Bradley, 2008), although Río de la Plata, Kalahari and Congo-São Francisco cratons were not considered as part of Rodinia (Kröner and Cordani, 2003; Cordani et al. , 2003; Tohver et al., 2006; Rapalini et al., 2013). Rodinia's time 1.1 to 0.8 Ga (Rogers and Santosh, 2003), ~ 1.2 to 0.9 Ga (McClellan & Gazel, 2014) and ~1.0 and ~0.75 Ga (Kröner, 2001) had been shortened in: (1) assembly between 1300 and 950 Ma, (2) supercontinent at 950 to 850 Ma, and (3) breakup between 850 and 600 Ma (Condie, 2003). The starting of Rodinia

breakup had been suggested along the western margin of Laurentia during 820 – 720 Ma (Hoffman, 1991; Powell et al., 1994; Li et al., 1999; Wingate & Giddings, 2000; Yoshida et al., 2003) Kalahari had been detached from Australia at 760 – 750 Ma (Yoshida et al., 2003). The breakup of Rodinia from 830 to 650 Ma, although some scientists recorded ~750 Ma for the starting time for its breakup and redistribution when the East Gondwana separated from the western margin of Laurentia leading to East and West Gondwana amalgamation in ~550 Ma (Weil et al. 1997). The breakup of this supercontinent indicated by the paired rift belts along continental margins, swarms of radial mafic dykes, which intruded neighboring continents, and Large Igneous Provinces (Bogdanova et al. 2009), such as the mantle super plume in South Australia (Wingate et al., 1998), South China (Li et al., 1999), Tarim (Lu et al., 2008), Kalahari (Frimmel et al., 2001), India (Radhakrishna and Mathew, 1996), and the Arabian–Nubian Craton (Stein and Goldstein, 1996). While the final stage of its breakup determined from opening of the Iapetus Ocean between 650 and 550 Ma (Cawood et al., 2001; Pisarevsky et al., 2008). These final processes associated with the Pan African Orogeny and by the formation of Gondwana supercontinent; the Braziliano, Adamastor, and Mozambique oceans convergence (Meert, Van der Voo, 1997; Collins, 2003; Pisarevsky, 2005; Pisarevsky et al., 2008; Bogdanova et al. 2009).

The assemblage processes of supercontinents are dominated by igneous intrusions that sourced from the mantle recording its source, nature and relationship between crust and mantle (Pearce et al., 1984, Kamber, 2015). Various mafic rocks represented in response to the convergence and divergence processes (Ernst et al., 1997, 2008; Ernst and Buchan, 2001; Mayborn and Lesher, 2004; Peng et al., 2007; Zhang et al., 2009; Goldberg, 2010; Hou, 2012; Ernst et al., 2013). The significance of these mafic intrusive rocks are in revealing the plate tectonics and recording the magmatic evolution within intra-oceanic arc systems (Burg, 2011; DeBari and Greene, 2011; Garrido et al., 2007) and evolved igneous intrusions (Rudnick and Gao, 2003; Leat and Larter, 2003; Tatsumi et al., 2008; Stern, 2010) and the Archaean continental crust growth distributions (e.g. Taylor and McLennan, 1995; Rudnick, 1995; Castro et al., 2013; Gazel et al., 2015). Sudan is famous in wide separate lenticular amphibolites lenses illustrating these metamorphosed mafic intrusions. The Red Sea opening and closing also generated the ophiolite of Jebel Rahib (Schandelmeier et al., 1990; Abdel-Rahman et al., 1990) and low-grade sedimentary belt in Kordofan. In central Sudan these Neoproterozoic rock sequences were intruded by granitoid rocks (Abdel Salam et al. 2002) and mafic rocks. The sequence evolution of the Red Sea Hills sector of the Nubian Shield are divided into three periods; the early period (1200-1000 Ma); the Middle period (1000-600 Ma) and Late Pan African period (600-500 Ma) (Abdel-Rahman, 1993), comparable with the events that supporting ophiolite-arc collision accretion model (Gass, 1981; Abdel-Rahman, 1993), which generally associated with igneous intrusive dominated by mafic rocks. In this paper, we investigated the geochemistry and petrography of amphibolites from Jebel Kordofan, El Obeid area, Sudan, to authenticate if they are ortho-amphibolites and will represent tholeiitic or calc-akaline basaltic protoliths. Moreover, we will discuss their tectonic environments and evolution and compare it with the global tectonics processes of Rodinia Supercontinent reconstruction during the Proterozoic period.

2. Geological background

The study area is located within the oldest and most extensive rock unit in whole Sudan. This unit which is known as Basement Complex consists of granites, gneisses, schists, quartzites crystalline limestone and other igneous and metamorphic rocks (Rodis, et al., 1964; Vail, 1973; Abdel Mageed, 1998; Mustafa, 2007). The oldest basement complex rocks known are the gneisses of Jebel Uweinat have ~2.9 Ga, some of them retrograded to ~2.6 Ga even with the younger one dated at ~1800 Ma (El Gaby, 1988). Generally, this unit is unconformably overland by Supracrustal metasediments comprized marbles, amphibolites, schists, and quartzites. Varies groups of the syn-to late-orogenic intrusions comprising granites and granodiorites with volcanic equivalents, sheared felsites and post-orogenic intrusions of granites and syenites intruded the basement complex unit (Mustafa, 2007). In Kordofan region the granitic or granodioritic gneisses are the dominant rocks of these basement south of Abu Gubeiha, near Abbasiya and near Jebel Dair where these rocks are distinguishable with their sedimentary origin. Graphitic schists and siltstones also recorded near Talodi and Kalogi, west of Rashad, east of Abbasiya and north of Abu Zabed. These basement units were intruded by gabbros northeast of Kalogi, granitic and syenitic intrusions masses in Jebel Dair, Jebel Dumbeir, Jebel Talodi and limon Hills and regional dykes of felsite and quartz veins trending E-W. Jebel Kordofan where these amphibolites collected represents an uplift block of Precambrian Basement rocks on the western side of the fault boundary of the Umm Rawaba basin (Vail, 1973; Mustafa, 2007). In Umm Badr-Sodari area these Basement complex rocks comprised weakly foliated grey biotite gneisses, granitic gneisses, pink augen gneisses with foliation trending N-S and subdominant N 30º E and Supracrustal sedimentary group including amphibolites, hornblende schist, graphitic schist, chlorite schist, micaceous quartzites, marbles, siliceous slates and metagabbros. These rocks intruded by syn- to late-orogenic granites south of Hamrat Esh Shiekh town, sheared felsitic extrusives and post-orogenic intrusions of granites and syenites with volcanic equivalents (El Khidir, 1997). In some parts the

low-lying Basement rocks of the Precambrian separated the sedimentary rift basins and sub-basins that encountered in the area and in other parts these basins had been separated by shallow seated basement rocks (Vial, 1978 & 1990). These rocks form an extended dome from the southeast to northwest through the central part of the area separating the two basins in the area from each other (Abadalla, 1999). The Basement rocks in the area are mainly amphibolite facies that mostly retrograde to green schist facies such as the Biotite and granitic gneisses that underwent migmatization in some parts (Rodis et al., 1964; Mustafa, 2007). Due to the lacking data and other reasons no emplacement ages obtained from these basements.

During the Neoproterozoic the formation time of the Arabian-Nubian Shield (ANS), East Saharan Craton (ESC) reworking in North Africa and the Mozambique Belt formation in Central and South Africa, the East African Orogen (EAO) formed in response to the mentioned events. The orogeny of EAO started with the breakup of the Rhodinia Supercontinent ~900-850 Ma reconstructing Gondwana Supercontinent. In response to Gondwana formation the juvenile crustal materials with abundant ophiolites in ANS generated due to the arc terrains accretion and amalgamation (Stern, 1994; El Khidir, 1997; Mustafa, 2007). Also the opening and closing of Red Sea formed the ophiolite in Jebel Rahib and low-grade sedimentary belt in Kordofan region in central Sudan due to. These rock sequences are intruded by the Neoproterozoic granitoids between 750 and 550 Ma (Abdel Salam et al., 2002). The Saharan Metacraton (Fig. 1) had been known as high- to medium-grade gneiss, metasediments, migmatites and pockets of granulite (Abdelsalam et al., 2002), that intruded by numerous migmatites and granitic gneiss which metamorphosed on amphibolite facies (Vail, 1971; Schandelmeier et al., 1987; Harms et al., 1990; Abdel-Rahman et al., 1990; Abdelsalam and Dawoud, 1991; Abdelsalam et al., 2002; Küster and Liégeois, 2001; Küster et al., 2008, Ibinoof et al. 2016).

3. Geology and petrography of the amphibolites

The amphibolites generally occurred in lenticular shapes as lenses within the Precambrian basements that represented by the gneisses and migmatites in J. Kordofan south east of El Obeid city and J. Kurbag, in the south part of the city these gneisses were found in J. Abu Uroug (Fig. 2). These gneisses unfortunately inexactly dated to define period, but they are of Precambrian age (Whiteman, 1971; Vail, 1973, 1978; Mustafa, 2007). The lenses of the amphibolites in J. Kordofan are varying from few meters and showing evidence of poly metamorphism, that they do not show any anatexis leucosomes on their outcrops. Three metamorphism cycles recorded in the area; the medium- to high-grade metamorphosed in amphibolite facies which affected the Pre-Cambrian units (late Archaean/ early Proterozoic) represented the first phase. The second one represented by the low-grade metamorphism in green schist facies which affected the old rocks and the Supracrustal sediments during the Saharan Metacraton reworking ended with Pan-African event (El Khidir, 1997; Mustafa, 2007). The third phase affected all units' sequences in the region and is also of green schist facies which has dynamic nature (El Algeed etal., 1981; Al Beily etal., 1986; El Khidir, 1997; Mustafa, 2007).

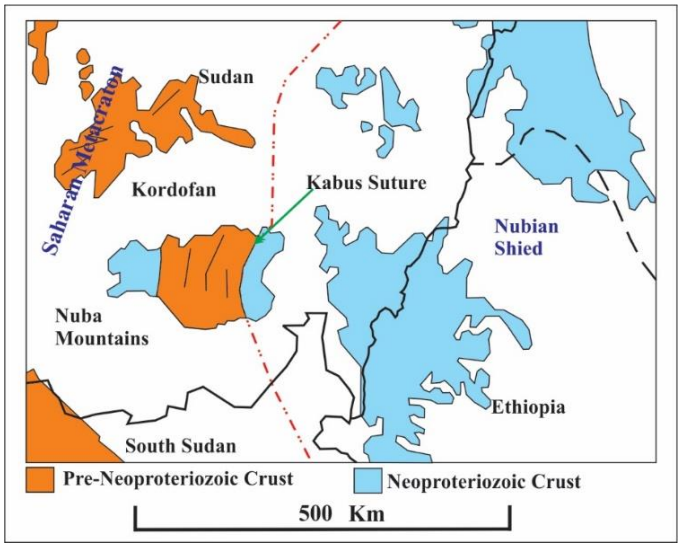

Fig. 1. The boundary of the Saharan Metacraton and Arabian Nubian Shield along the Study area (the blue line). (Modified after Abdelsalam et al., 2002; Ibinoof et al., 2016).

The amphibolites of J. Kordofan lack any anataxis or leucotomies where they cropped out, they are black in colour showing gneissic structures and medium to coarse-grained textures (Fig. 3a, b), dominantly composed of Hornblende (55-65 %), Plagioclase (15-25 %), Quartz (~5%), and aggregates of epidote and plagioclase, suggesting medium-grade metamorphism of amphibolite facies. The opaque minerals are also present as accessories, specially iron oxides and apatite.

4. Sampling and analytical methods

A total of 8 fresh samples from J. Kordofan amphibolites were collected for geochemical analysis including major and trace elements, whole-rock Sr and Nd isotopes. These samples prepared through crushing by a steel mortar, and then ground an agate mill to less than 200 meshes. Measuring the abundances of the major and Trace element had been conducted in the State Key Laboratory of Geological Processes and Mineral Resources, China University of Geosciences Wuhan by the XRF–1800 and ICP-MS on an Agilent 7500a. Accuracies of the major elements for the XRF analyses are estimated to be 1% for SiO_2 and 2%, for the trace elements. ICP-MS analyses procedures following Liu et al. (2008) and they yield accuracies better than 5%.

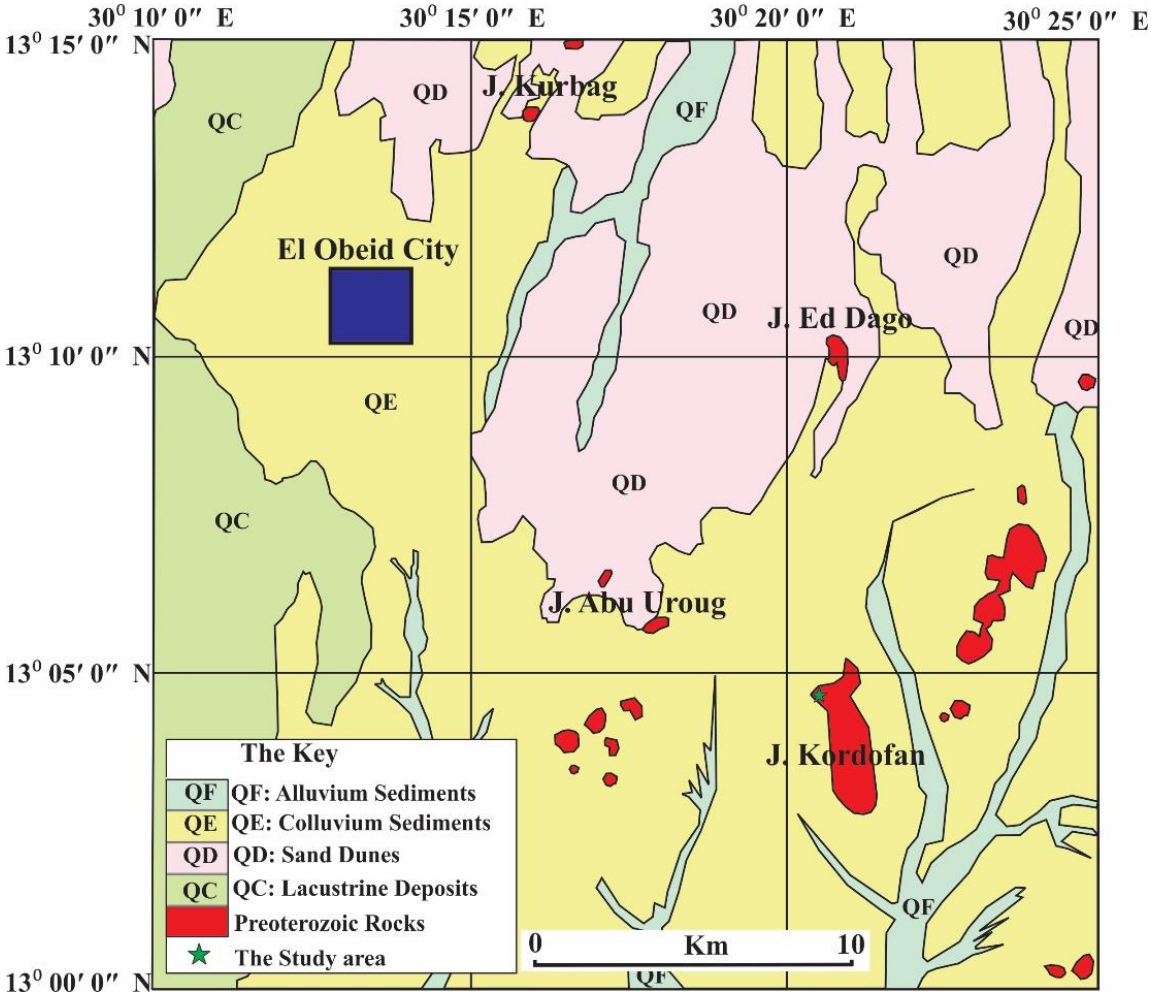

Fig. 2. Geological map of the El Obeid area showing the study area and the rock units (modified after Geological Research Authority of Sudan GRAS 2017).

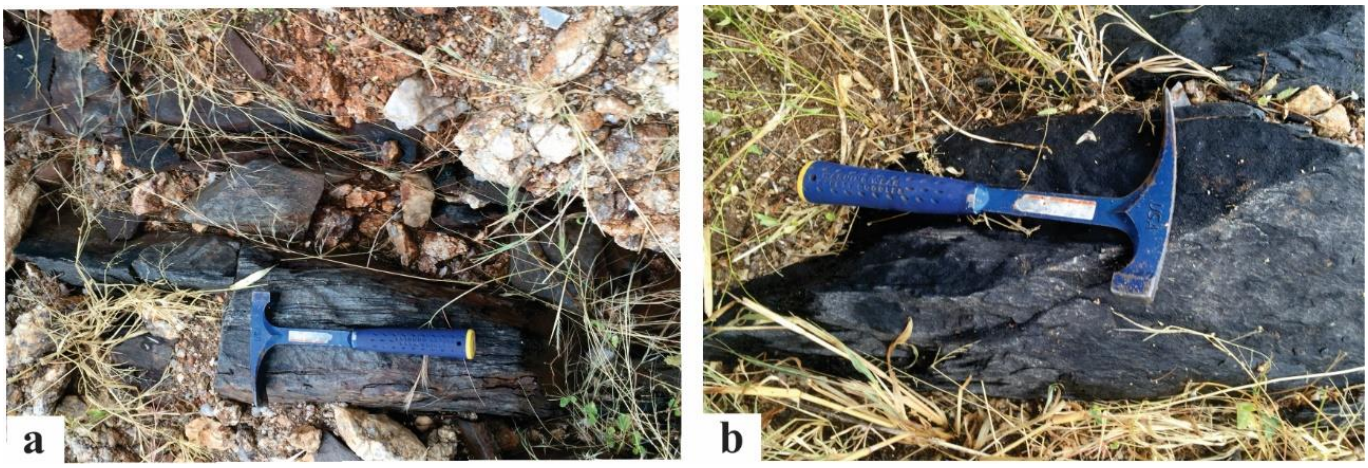

Fig. 3. Photographs for amphibolites in the study area showing bedding gneissic structures without anatexis leucotomies.

5. Results

5.1 Whole-rock major and minor element geochemistry

The results of the major and trace element for the amphibolites from J. Kordofan from El Obeid area, North Kordofan, Sudan are listed in Table 1. These amphibolites contain LOI values of less than 2.00 wt% with narrow alteration interval ranging from 0.69 to 1.50 wt%, suggesting weak alteration from the fluid on these rocks.

Table 1. Major and trace elements of the amphibolite from Jebel Kordofan from El Obeid area

Sample	16HK1	16HK2	16HK3	16HK4	HK5	HK6	HK7	HK8
Major oxides (wt %)								
SiO_2	47.2	50.3	50.7	50.5	46.7	47.0	47.0	50.6
TiO_2	2.43	1.54	1.57	1.62	2.60	2.06	1.98	1.56
Al_2O_3	17.0	14.6	14.4	14.8	15.4	16.0	13.7	14.0
TFe_2O_3	12.4	13.6	13.8	13.8	13.2	12.4	13.5	14.0
MgO	6.03	7.64	7.60	7.32	5.69	6.83	7.91	6.94
MnO	0.19	0.22	0.22	0.22	0.19	0.15	0.18	0.22
CaO	13.5	10.4	10.2	10.2	14.4	14.1	14.7	11.2
Na_2O	0.67	1.27	1.08	1.06	1.19	0.77	0.57	1.02
K_2O	0.25	0.31	0.28	0.29	0.27	0.30	0.24	0.35
P_2O_5	0.34	0.12	0.13	0.13	0.31	0.44	0.23	0.13
LOI	1.10	0.86	0.80	0.93	0.92	1.50	1.09	0.69
Total	101.1	100.9	100.8	100.9	100.9	101.5	101.1	100.7
$Mg^{\#}$	46.7	50.4	49.8	48.8	43.6	49.8	51.4	47.2
Trace elements (ppm)								
Sc	27.2	63.0	63.4	60.1	33.4	30.1	29.4	43.7
V	333	347	355	355	338	251	270	334
Cr	186	127	119	118	187	838	499	119
Co	48.2	52.6	53.8	55.5	44.5	68.7	54.6	49.4
Ni	80.5	55.3	53.5	54.7	79.1	500	222	53.7
Rb	12.1	5.90	5.10	4.90	6.52	20.2	13.4	11.9
Sr	511	100	100	101	500	347	313	101
Y	27.0	33 .0	35.0	35.0	27.8	22.6	20.3	33.1
Zr	171	87.5	93.8	99.0	156	135	115	87.9
Nb	13.0	2.00	2 .00	3.00	18.7	15.4	15.1	3.01
Ba	14.7	11.5	9.35	9.98	31.9	10.8	17.1	15.1
La	13.0	5.94	5.99	6.18	17.0	14.1	14.2	4.29
Ce	40.0	7.20	7.40	7.80	39.1	32.3	31.9	12.2
Pr	5.4	2.00	2.00	2.10	5.07	4.38	4.20	1.88
Nd	27.1	11.8	12.5	12.7	23.4	19.3	18.9	10.1
Sm	5.55	3.41	3.53	3.61	5.68	4.69	4.77	3.58
Eu	1.77	1.16	1.23	1.21	1.88	1.60	1.49	1.19
Gd	5.44	3.98	4.18	4.20	5.48	4.71	4.42	4.57
Tb	0.92	0.83	0.87	0.87	0.89	0.76	0.72	0.85
Dy	5.32	5.61	5.89	5.96	5.30	4.37	4.11	5.67
Ho	1.01	1.21	1.26	1.27	1.03	0.84	0.75	1.22
Er	2.79	3.47	3.70	3.74	2.71	2.19	1.95	3.40

Tm	0.42	0.58	0.61	0.61	0.38	0.32	0.28	0.52
Yb	2.44	3.50	3.69	3.67	2.42	1.91	1.65	3.44
Lu	0.36	0.53	0.56	0.56	0.36	0.27	0.23	0.49
Hf	4.22	2.44	2.58	2.71	3.93	3.45	3.04	2.58
Ta	1.42	0.26	0.28	0.28	1.15	0.92	0.94	0.23
Pb	6.05	3.48	3.97	4.00	5.94	6.32	2.98	3.21
Th	1.62	0.53	0.53	0.57	1.50	1.23	1.22	0.53
U	1.270	0.140	0.150	0.160	0.84	0.97	0.58	0.15
Ratios								
Ba/Nb	1.10	5.02	3.77	3.82	1.71	0.70	1.14	5.02
La/Nb	0.97	2.59	2.42	2.37	0.91	0.92	0.94	1.43
Th/Nb	0.12	0.23	0.21	0.22	0.08	0.08	0.08	0.18
Th/Ta	1.14	2.04	1.89	2.04	1.30	1.33	1.30	2.31
La/Ta	9.20	22.8	21.4	22.1	14.8	15.3	15.1	18.8
La/Yb	5.33	1.70	1.62	1.68	7.03	7.40	8.61	1.25
Zr/Nb	12.8	38.2	37.8	37.9	8.4	8.8	7.6	29.3
Zr/Sm	5.55	3.41	3.53	3.61	5.68	4.69	4.77	3.58
Zr/Hf	40.5	35.9	36.4	36.5	39.8	39.2	37.8	34.1
Lu/Hf	0.09	0.22	0.22	0.21	0.09	0.08	0.08	0.19
Ba/Zr	0.09	0.13	0.10	0.10	0.20	0.08	0.15	0.17
Eu/Eu*	0.97	0.96	0.97	0.94	1.01	1.03	0.97	0.89
Ti/V	18.2	20.9	21.3	21.4	18.3	20.2	16.7	21.9
(Hf/Sm)n	1.09	1.03	1.05	1.08	1.00	1.06	0.92	1.03
(Ta/La)n	1.83	0.73	0.78	0.76	1.14	1.09	1.11	0.89
(La/Th)n	0.99	1.39	1.40	1.34	1.41	1.43	1.44	1.01
(La/Ce)n	0.84	2.15	2.10	2.06	1.12	1.13	1.15	0.91
(La/Yb)n	3.82	1.22	1.16	1.21	5.05	5.31	6.18	0.90
TFeO = 0.8998TFe2O3, Mg# = [100(MgO/40.3)]/[MgO/40.3+FeO/71.8], Eu/Eu* = (Eu)cn/[(Gd)cn								
+ (Sm)cn]/2, cn- chondrite normalized; n-primitive mantle normalized.								

These amphibolites have silica content ranging from 46.7 to 50.7 wt% indicating typically mafic or basic rocks, their alumina contents ranging from 13.7 to 17.0 wt%. These rocks have enrichment of TFe_2O_3 ranging from 12.4 to 14.0 wt%, TiO_2 ranging from 1.54 to 2.60 wt% and the contents of CaO which range from 10.2 to 14.7 wt%, but they characterized by very low contents of P_2O_5 values which ranges from 0.12 to 0.44 wt%, Na_2O 0.57 to 1.27 wt%, K_2O contents are range from 0.25 to 0.35 wt%, with total alkali of (0.81–1.58 wt%), MgO ranging from 5.69 to 7.91 and the $Mg^{\#}$ for these amphibolites varies from 43.6 to 51.4. Plots on MgO–CaO–Fe_2O_3 (major elements only) discriminated these rocks as ortho-amphibolite (Fig. 4a) and plot on Zr–MgO diagrams, also discriminated them as ortho-amphibolite, suggesting basaltic precursor magmas for their protoliths (Fig. 4b).

Harker diagram for these amphibolites that correlated some major and trace elements with MgO, show negative correlations of CaO, TiO_2, P_2O_5, Cr, Co and Al_2O_3 with MgO (Figs. 5c, d, f, g, i), and positive correlations of Fe_2O_3 and Ni with MgO (Figs. 5a,h); while Na_2O show un obvious correlations with MgO (Figs. 5b,e). On TAS (Total Alkalis vs silica) that uses major elements, these amphibolites discriminated as sub-alkaline basalts (Fig. 6a). In Zr/TiO_2 *vs.* Nb/Y diagrams which used both major and trace elements indicated andesite to andesitic basalts for the protolith of these rocks (Fig. 6b), suggesting silicate mobilization in these amphibolites. These rocks showed Tholeiite affinities in the AFM plot of Irvine and Baragar (1971) (Fig. 7a), but showed Calc-alkaline to Tholeiitic affinities on TiO_2 *vs.* FeO*/MgO diagram due to their low TiO_2 contents (Fig. 7b).

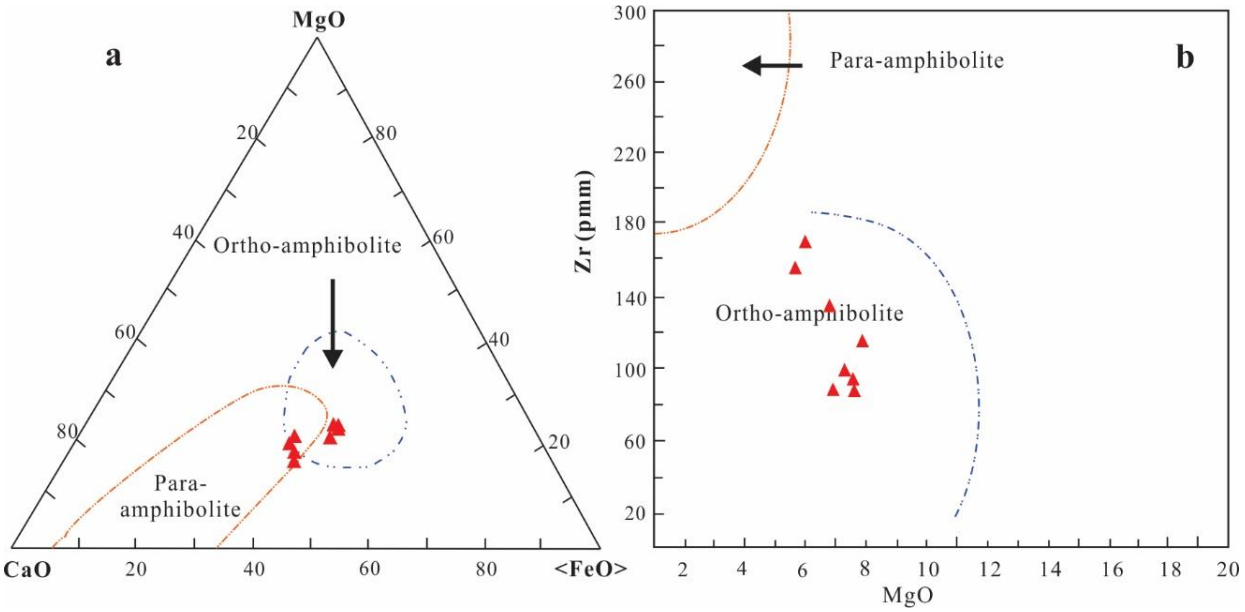

Fig. 4. MgO – CaO – Fe_2O_3 and Zr vs MgO discrimination diagrams of Walker et al. (1960) and Geringer, (1979), respectively, for amphibolites from J. Kordofan in El Obeid area.

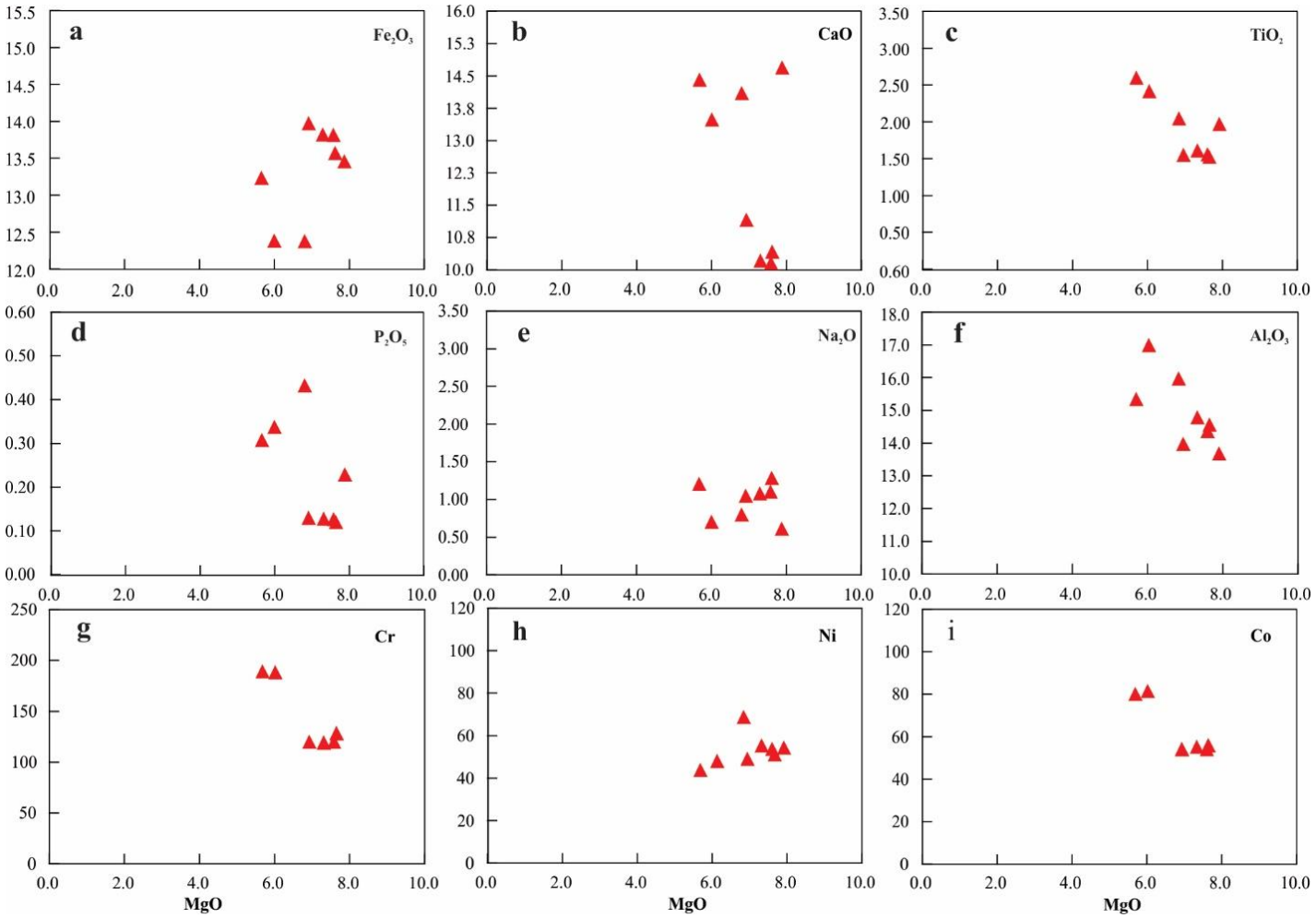

Fig. 5. Harker diagrams using MgO vs. some major and trace elements for amphibolites from J. Kordofan in El Obeid area (major oxides have been normalized to 100% anhydrous). Symbols are the same as those in Fig. 4.

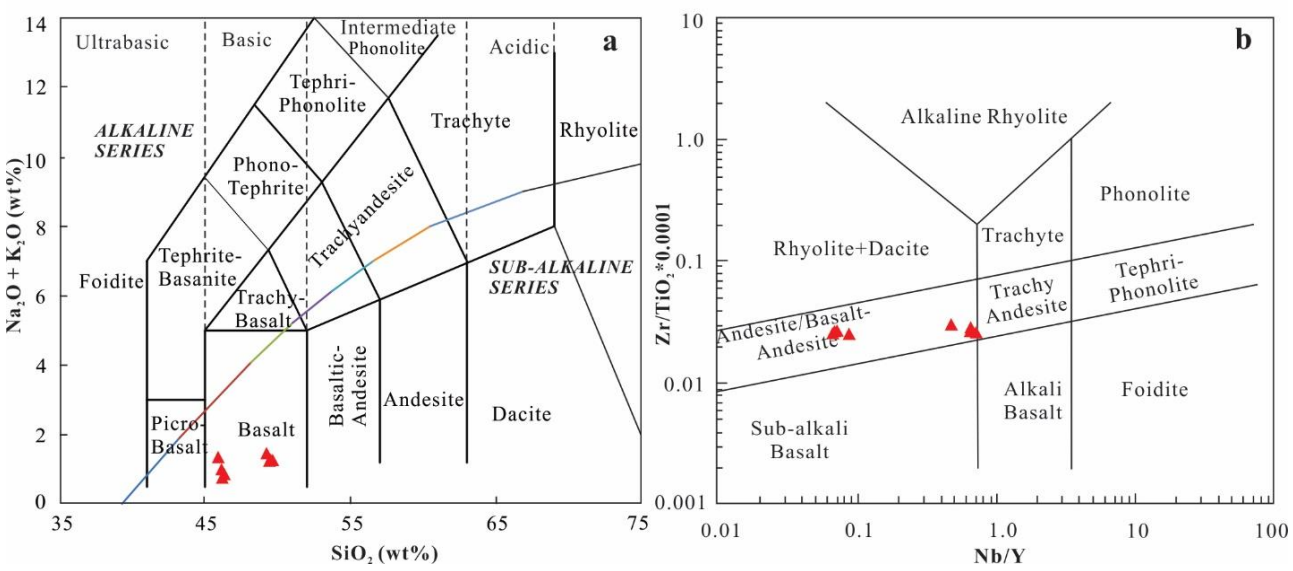

Fig.6. (a) TAS of Lebas et al. (1986), (b) Zr/TiO_2 vs. Nb/Y of Pearce (1996) diagrams for amphibolites from J. Kordofan in El Obeid area. Symbols are the same as those in Fig. 4.

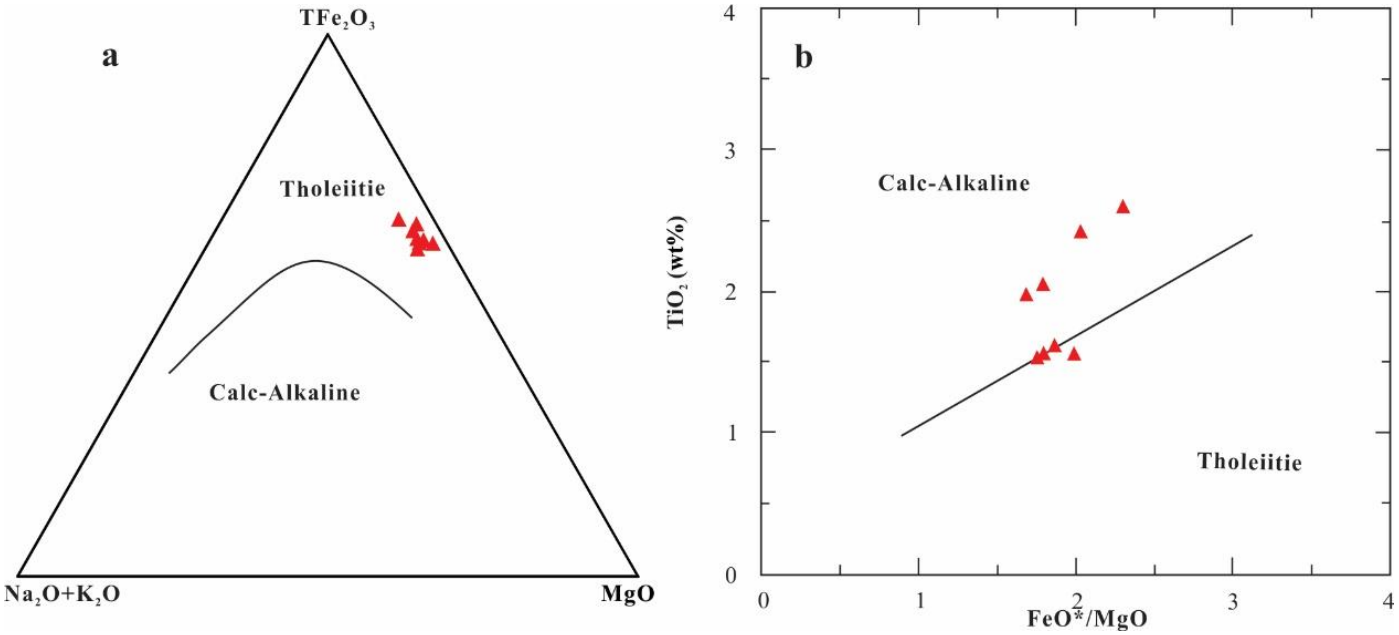

Fig. 7. (a) AFM diagram of Irvine and Baragar (1971). (b) TiO_2 vs. Fe*/Mg of (Miyashiro et al., 1975) for amphibolites from J. Kordofan in El Obeid area. Symbols are the same as those in Fig. 4.

These amphibolites characterized by low values of Ni ranges from 53.3 to 500 ppm, Co value ranges from 44.5 to 68.7 and Cr value ranges from 118 to 838 ppm, these elements have varied correlation with MgO (Figs. 5g, h, i) suggesting evolved protoliths magma nature for these rocks (Ahijado et al., 2001). These rocks also have Zr/Hf ratios ranging from 34.1 to 40.5 and have Ti/V values range from 16.7 to 21.9. These amphibolites are characterized by similar chondrite-normalized REE patterns (Fig. 8a), their ΣREE contents ranges from 51.1 to 11.5 ppm, with slight depletion of LREE relative to HREE ($(La/Yb)_n$ = (0.90–6.18) and positive to negative Eu anomalies (Eu/Eu* = 0.89–1.03). These amphibolites on the primitive mantle normalized incompatible-element spider diagram, characterized by slightly enrichment of LILE (Rb, Ba, U), with strongly positive P, negative Ti, Zr–Hf and an obvious Nb–Ta anomalies displaying significant spiky patterns (Fig. 8b). The contents of Nb on these samples ranging from 2.00 to 18.7 ppm and values for the Nb/La and Nb/U ratios ranging from 0.39 to 1.10 and 10.6 to 26.1, respectively, when plotted on related discriminations diagram they discriminated as a Nb-rich island

arc basalt with an island arc basalts affinities (Fig. 9a, b). The Nb-enrichment basaltic rocks are usually dominated with the partial melting in metasomatized mantle wedge in subduction zone environments (Defant et al., 1992; Sajona et al., 1996; Taylor and Nesbitt, 1998; Hollings and Kerrich, 2000; Cai et al. 2014; Mazhari et al. 2016), as well as heterogeneous depleted and enriched mantles (Petrone and Ferrari, 2008).

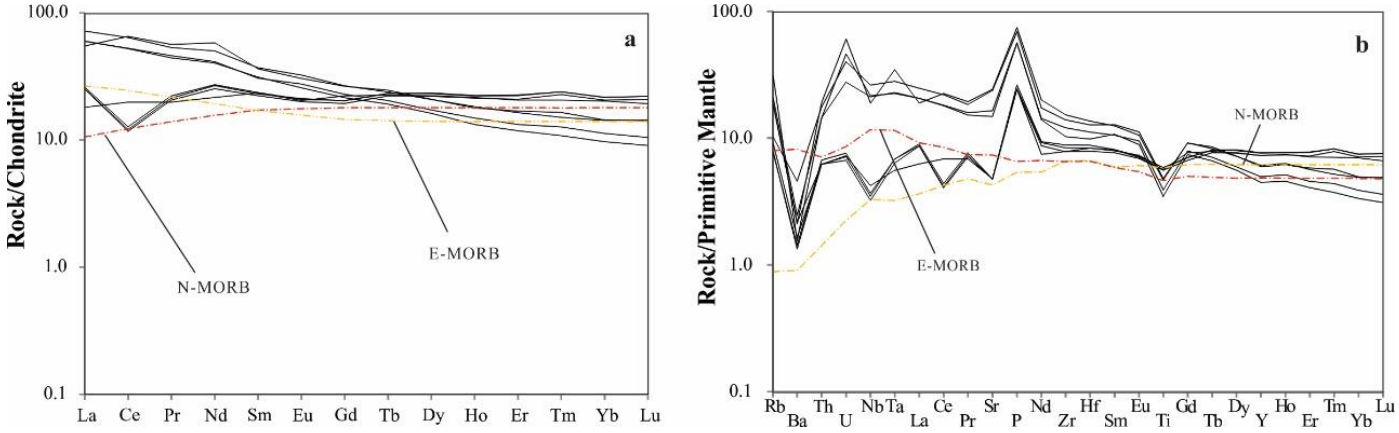

Fig. 8. (a) Chondrite-normalized REE diagram (b) primitive mantle-normalized incompatible-element Spider diagram for amphibolites from J. Kordofan in El Obeid area. The normalization values of chondrite and primitive mantle and the data for Ocean Island Basalt (OIB), Normal Mid-Ocean Ridge Basalt (N-MORB), Enriched Mid-Ocean Ridge Basalt (E-MORB) are from Sun and McDonough (1989).

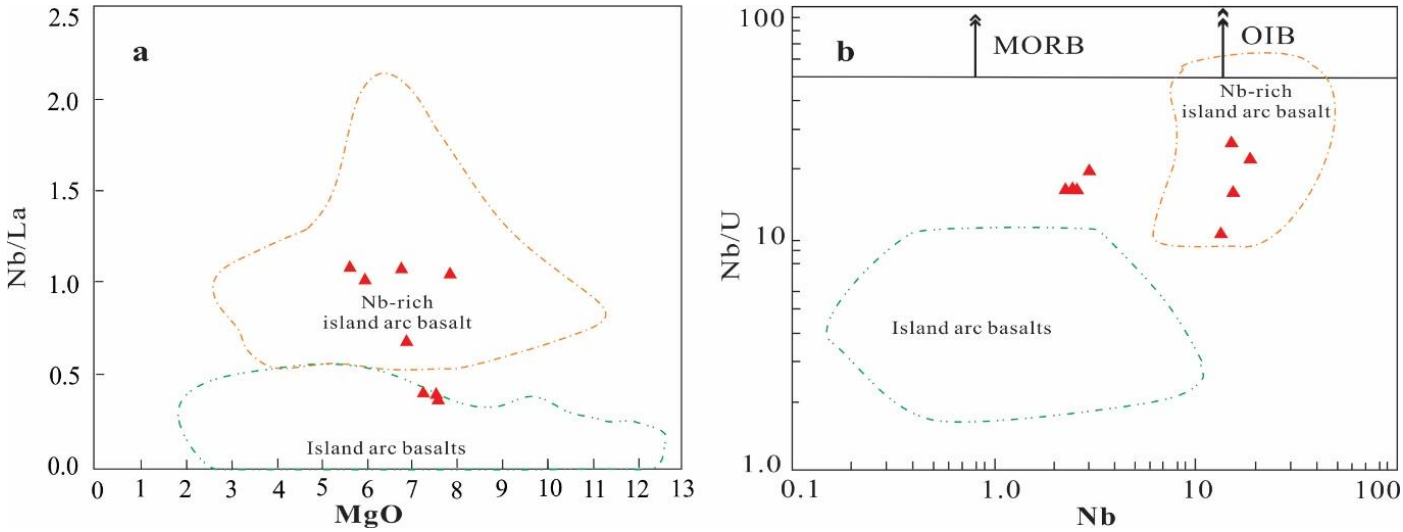

Fig. 9. Nb/La vs Mgo and Nb/U vs Nb diagrams of Kepezhinskas et al. (1997) for amphibolites from J. Kordofan in El Obeid area. Symbols are the same as those in Fig. 4.

6. Discussion

In conditions of the amphibolite-facies metamorphism, the alkali elements Na and K and some other incompatible elements including Large Ion Lithophile Elements (LILEs), such as Rb, Ba, Th and U and light rare earth elements LREEs as well as Sr and Pb become immobile thus changes in response to their non-stability (Cullers et al., 1974; Rollinson, 1993 Staudigel et al., 1995; Ahmed-Said and Leake, 1997; Kelley et al., 2003; Xiao et al., 2013). The studied amphibolites occurred within the gneisses and migmatites in Kordofan region, El Obeid area that metamorphosed on the same conditions, discrimination diagrams for vast of these rocks are also confirm the incompatible LILEs, so for our discriminations and investigations we will not depend on only these mobile elements to discuss the petrogenesis and tectonic implications.

6.1 Formation time Constraint for the protoliths of the amphibolites

The first choice for constraining the time of the emplacement of the precursor magmas and metamorphism is zircon U-Pb geochronology (magmatic or/and metamorphic zircons). These amphibolites have been metamorphosed to amphibolite facies temperature conditions, no magmatic zircons or metamorphic or/and anatexis genetic zircons preserved for their protoliths, so the whole-rock Sm-Nd isochron dating which is also considered to constrain the formation age of the protoliths of the

amphibolites, unfortunately also no such data preserved for these rocks yet. In case of neither magmatic zircon dating nor whole-rock Sm-Nd isochron modeling, we discussed the formation age interval to constrain the youngest age of the detrital zircons and the oldest metamorphic age and the intrusive age in the area or for whole region.

Amphibolites from Jebel El Eiza'a in El Obeid area North Kordofan western Sudan about 10 km to the north of these amphibolites yielded LA-ICPMS U-Pb age of 997 Ma for their magmatic zircons with lower intercept ages of 403 ± 130 Ma and upper intercept ages of 1020 ± 74 Ma. In Bayouda area northern central Sudan inherited zircon grains also yielded LA-ICPMS U-Pb age of 895, 917, 946 and 999 Ma, while magmatic zircons yielded an average age of 794±15 Ma (Evuk, 2013). Metagranite zircon core grains from Abu Harik and Kurmut Terranes yielded ages of 969±5 Ma and 914.1±5.5 Ma, while some yielded ages of 842, 843 and 851 Ma (Evuk, 2013). Inherited zircons from Rahaba-Absol Terrane are also recorded Paleoproterozoic ages of 1617 to 2281 Ma and Mesoproterozoic ages of 1007 to 1434 Ma (Evuk, 2013). In Nuba Mountains the Low-grade metavolcanic rocks yielded Sr–Nd isochron age of 778 ± 90 Ma represented an oceanic arc/back- arc assemblage similar to those of arc the Arabian Nubian Shield with a little or no involvement of older materials having an age of 814 Ma (Ibinoof et al. 2016). A new study proposed magmatic zircons from carbonatites and granites from Jebel Dumbeir and Jebel Ed Dair yielded LA-ICPMS U-Pb age of 560 and 605 Ma. The alkaline -carbonatite complex of Jebel Dumbier and most A-type granites of the Arabian-Nubian Shield, indicated the magmatisms of the post-orogenic alkaline during the final Pan-African orogen evolution at ~ 650-550 Ma (Wang et al., 2017).

The above discussion of the zircons U-Pb obtained from Bayouda area rocks linked to the tectonic evolution of the whole Sudan, and the geological field observations and petrographical evidences from these amphibolites and correlation with older and younger rocks in the region. Consequently, and reasonably we considered the timing of emplacement of precursor magmas of the protoliths of these amphibolites are between ~1020 and ~778 Ma.

6.2 Petrogenesis

6.2.1 Magma crystallization and differentiation

Fractional crystallization of some minerals (e.g. olivine and pyroxene) in magma chamber before ascending and intruding can be distinguished from their low MgO, $Mg^{\#}$ and trace elements (eg. Co, Cr and Ni etc) and this indicate evolved magmas rather than primary melts (Ahijado et al., 2001). Furthermore, for authenticating the crystallization differentiation the correlation of some major and trace elements with MgO of Harker diagram are useful and support this process (Fig. 5), as well as Eu anomalies in the Chondrite-normalized REE patterns (Fig. 8). The studied amphibolites characterized by very low MgO (5.69-7.91 wt%), Mg# (43.6-51.4), Ni (53.5-500 ppm), Co (44.5-68.7) and Cr (118-838), showing negative correlations of P_2O_5 and Al_2O_3 with MgO (Figs. 5d, f), while showing positive correlations of Fe_2O_3, CaO, Cr, Ni and Co (Figs. 5a, b, g, h, i); and un obvious correlations of TiO_2 and Na_2O (Figs. 5e, c). These variable correlations of major and trace elements, definitely suggest insignificant plagioclase fractional differentiation (Figs. 5). These amphibolites displayed relatively flat distributions chondrite-normalized rare earth element patterns that characterized relatively by negative and positive Eu anomalies (Eu/Eu* = 0.97-1.03), with LREE enrichment (Fig. 8). The variable correlation of total FeO, TiO_2 and P_2O_5 with MgO (Figs. 5) may consider Fe–Ti rich-minerals such as apatite, magnetite and ilmenite in the evolved magma for these amphibolites. Generally, the low contents of SiO_2 (46.7-50.7 wt%), P_2O_5 (0.12-0.44 wt%) and high TiO_2 content (1.54-2.60 wt%) for these rocks, may discriminate them as ferrobasalts when correlated to the typical rocks, they have iron enrichment (FeOt = 12.3-13.8 wt%), (e.g. Wager, 1960; McBirney and Naslund, 1990; Xu et al., 2003; Wang et al., 2007; Zhang et al., 2012).

6.2.2 Crustal contamination

Crustal contamination by continental curst during crystallization in magma chamber is reasonable to the mantle sources. Many factors may cause negligible assimilation or crustal contamination to the precursor magma of the final derived rocks; such as; geological and petrographic evidences; the primitive mantle normalized incompatible elemental patterns of these rocks; the Zr-Hf troughs; the differentiation trend they displayed; and any others criteria. Through geological observations on the outcrops of these amphibolites contain many varies scale quartzite enclaves within the granitic and pegmatitic gneisses (Fig. 3a); These amphibolites displayed significant spiky patterns in the primitive mantle normalized incompatible-element spider diagram, enrichment of LILE, positive P, negative Ti anomalies, and diverse Nb–Ta and Zr–Hf troughs. In addition, they displayed Fenner-like trend (Fenner, 1929, not shown) indication of some minerals fractionation in low Oxygen fugacity conditions in the magma chamber e.g. olivine, plagioclase, pyroxene, etc…, so the precursor magma these amphibolites cause negligible crustal contamination. Over all, the whole-rock geochemistry restricted the crustal assimilation and contamination during magma differentiation as considered by some values and ratios. These amphibolites characterized by FeO_t contents of (>10 and <20 wt%) and TiO_2 (>1.00,

mostly >1.50 wt%) are quietly vary from the rocks from the upper crust (Rudnick and Fountain, 1995; Taylor and McLennan, 1985) and also differ from the amphibolite rocks in Jebel El Eiza'a that formed prior to them in the region, which have contents of FeO_t (<10 wt%) and TiO_2 (>0.51, mostly >0.61), and the Neoproterozoic amphibolites in Bayouda area which characterized by FeO_t content of 15.5 – 38.2 wt% and TiO_2 content 0.20–3.70 wt% (Evuk, 2013). These amphibolites slightly characterized by low ratios of $(Nb/La)_n$ which ranging from 0.37 to 1.06. Generally during magma ascending the LREEs and LILEs were increased with crustal contamination, which made some ratios such as Th/La and Nb/La useful for crustal assimilation and contamination indicators (Wang et al., 2007), these ratios are constant when the melts undergoing singly fractional differentiation. The geological and petrographical investigations that done on these amphibolites and so all geothermal interpretations, the crustal contamination to their precursor magmas during crystallization from the magma chamber can't not be excluded.

6.3 Mantle source nature

Through our field and geochemical investigations using the incompatible element we assumed and confirm the mantle natures and sources even the characteristics of where the basaltic magmas can be generated. Taking into our consideration that crustal materials contamination to the precursor magmas of these rocks occurred. The sources of the basaltic magmas dominantly come from asthenospheric mantle and/or lithospheric mantle. Rocks come from the asthenospheric mantle generally have oceanic island basalts (OIB) like-primitive mantle-normalized trace element patterns, with enrichment of LILE and positive HFSE or without Nb-Ta anomaly. In contrary, rocks that come from the lithospheric mantle wedge have typically like of arc patterns showing enrichment of LREE and LILE with negative Nb-Ta, Zr-Hf and Ti anomalies (Zou et al., 2000; Sklyarov et al., 2003; Zhao et al., 2007). The Nb-Ta negative anomaly also is another indication for crustal contamination, but easily can be separated by its positive Zr-Hf anomalies (Zhao et al., 2007; Zhao and Zhou, 2009).

Zr/Nb values for most of these amphibolites are higher than that of the OIB they are all >10 and only three samples are <10, but also higher than of OIB (Table 1), evidently (OIB = 5.83, Zhao, 2010) eliminating these amphibolites from the asthenospheric mantle origin rocks. Nevertheless, these amphibolites characterized by slightly enrichments in LREE and LILE but with HFSE (e.g., Nb, Ta, Zr and Hf), and dominantly negative Nb-Ta and Zr-Hf troughs in primitive mantle normalized incompatible element patterns, indicating an arc-related mantle for their precursor basaltic magmas.

Also, some incompatible elements ratios such as La/Ta, Th/Ta, La/Yb, Ba/Nb and La/Nb, etc. for these rocks displayed little partial fractional crystallization due to their similar distribution coefficients. Correlation of some these ratios, such as Th/Ta vs. La/Yb and Ba/Nb vs. La/Nb will show different mantle sources and trajectory (e.g. Condie, 1977). These amphibolites occurred with old rock units in their outcrop (gneisses and migmatites), which simply point to their precursor magmas origin that consequently derived from an old lithospheric mantle. Moreover, their enrichment of LILEs and LREEs, depletion in HFSEs and low values of $(Nb/La)_n$ and $(Nb/Zr)_n$ indicated the precursor magmas of these amphibolites come from a mantle source subjected to metasomatism by subduction melts (Wang et al., 2007; 2008b). Generally, Magmas with high La/Ta values (>30) reflected a typical sub-continental lithospheric mantle source that affected by enrichment of fluids and/or melts from subducted slab-derived during an old tectonic events (Thompson and Morrison, 1988). These amphibolite have La/Ta values range from 9.20 to 22.8, La/Nb values range from 0.91 to 2.59 and Ba/Nb values range from 0.70 to 5.02, proposing an enriched sub-continental lithospheric mantle source (Zhao et al., 2010). In addition, these rocks characterized by low $(Ta/La)_n$ but high $(Hf/Sm)_n$ ratios, discriminated them to a mix mantle sources influenced by injection of subduction-related melts (Fig. 10a,b,c). Finally, through our all investigations we can conclude that precursor basaltic magmas of J. Kordofan amphibolites were derived from a sub-continental lithospheric mantle source that metasomatized by subduction-related melts.

6.4 Tectonic settings

The amphibolites have basaltic precursor magmas protolith that will reveal important facts on their tectonic settings. They were tholeiitic to calc-akaline basalts (Figs. 6 and 7) indication of basaltic volcanism of primitive to more mature oceanic convergent margin of oceanic island arc and/or back-arc setting (Küster and Liegeois, 2001). These amphibolites displayed primitive mantle-normalized incompatible element patterns (Fig. 8b) typical of an arc basalts or island arc tholeiites (Mcculloch and Gamble, 1991; Francalanci et al., 1999) related to a subduction tectonic setting. The geochemical investigations and related tectonic settings indicators and discriminators for basalts had been done to identify their tectonic settings. The value of Zr/Sm for the arc basalts are generally lower than the chondritic value (~25) (Sun and McDonough, 1989) Aleutian arc-like basalts characterized by of ~20 (Mcculloch and Gamble, 1991), the Zr/Sm average in intra-plate basalts usually >25, while the lower, middle and upper crusts dominantly have the highest values of Zr/Sm that range from 24 to 42. The continental crust characterized by an average of 34 (Rudnick

and Gao, 2003; Zhou, 2007).

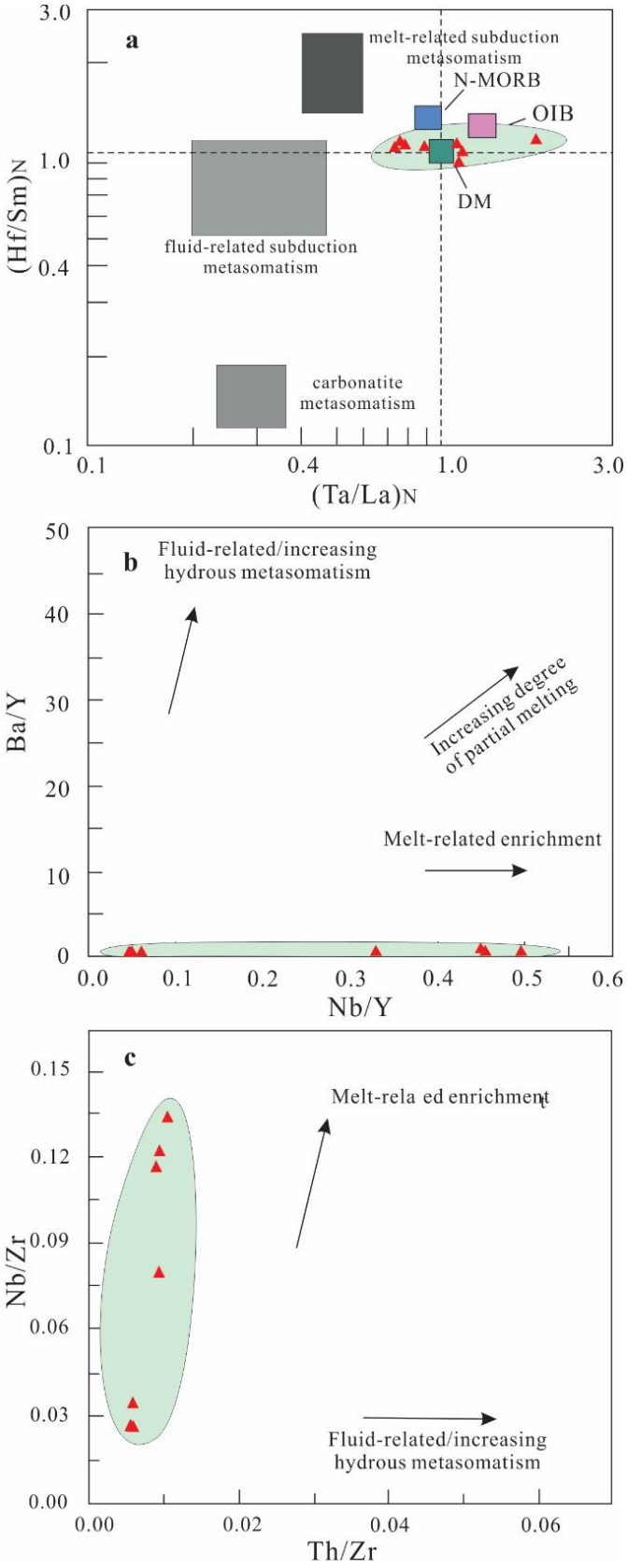

Fig.10. The diagrams of (a) (Hf/Sm)N vs. (Ta/La)N, (b) Ba/Y vs. Nb/Y, (c) Nb/Zr vs. Th/Zr (after Wang et al., 2007) for amphibolites from J. Kordofan in El Obeid area. Ranges of different sources in (a) are after (Hofmann and Jochum, 1996 and LaFle`che et al., 1998). While the range and trend shown in (b–c) are from Hofmann and Jochum (1996), Kepezhinskas et al. (1997) and Sobolev et al. (2000), respectively. Symbols are the same as those in Fig. 4.

The studied amphibolites showed arc basalts values characterizing by values of Zr/Sm range from 3.41 to 5.68 (Table 1), confirming that their precursor magmas and tectonic setting generated in an arc setting. On the plots of Nb*2 – Zr/4-Y and Zr/Y-Zr diagrams of (Pearce and Norry, 1979), these amphibolites are discriminated as within plate basalts, IAT and MORB (Figs. 11a, b), while on the plots of Hf/3-Ta-Th of (Wood, 1980) and Ti/100-Zr-Y*3 diagrams (Figs. 11c, d), they are further discriminated to be of island arc tholeiite (IAT), E-MORB and within plate basalts (WPB). Generally, we can assume those theses amphibolites suggesting within plate basalts, Island Arc Tholeiite, and Mid-Oceanic Ridges (MORB) affinities.Ti/V value is also useful for discriminating tectonic settings of basalts (e.g. Foster, 1994), its value in Island arc basalts typically are <20. The Ti/V values vary in MORB, back arc and the within-plate basalts that range from 20 to >50, the within-plate basalts can distinguish by their higher Ti, V and Zr contents. J. Kordofan amphibolites showed values of Ti/V range from 16.7 to 21.4, discriminating their precursor magmas typical of MORB, back arc and island arc basalts excluding them from within-plate basalts, because they characterized by low Ti, V and Zr contents. Plots on TiO_2 vs Zr of Pearce and Cann (1973) and V vs Ti/1000 of Shervais (1982) (Fig 12a, b) shows that these amphibolites were arc and back arc basalts. So for determining the tectonic settings for these amphibolites, we investigated their primitive mantle-normalized incompatible element patterns and some typical indicators for tectonic settings of basalts, which all indicated that the precursor magma of these amphibolite have an arc and back arc affinities.

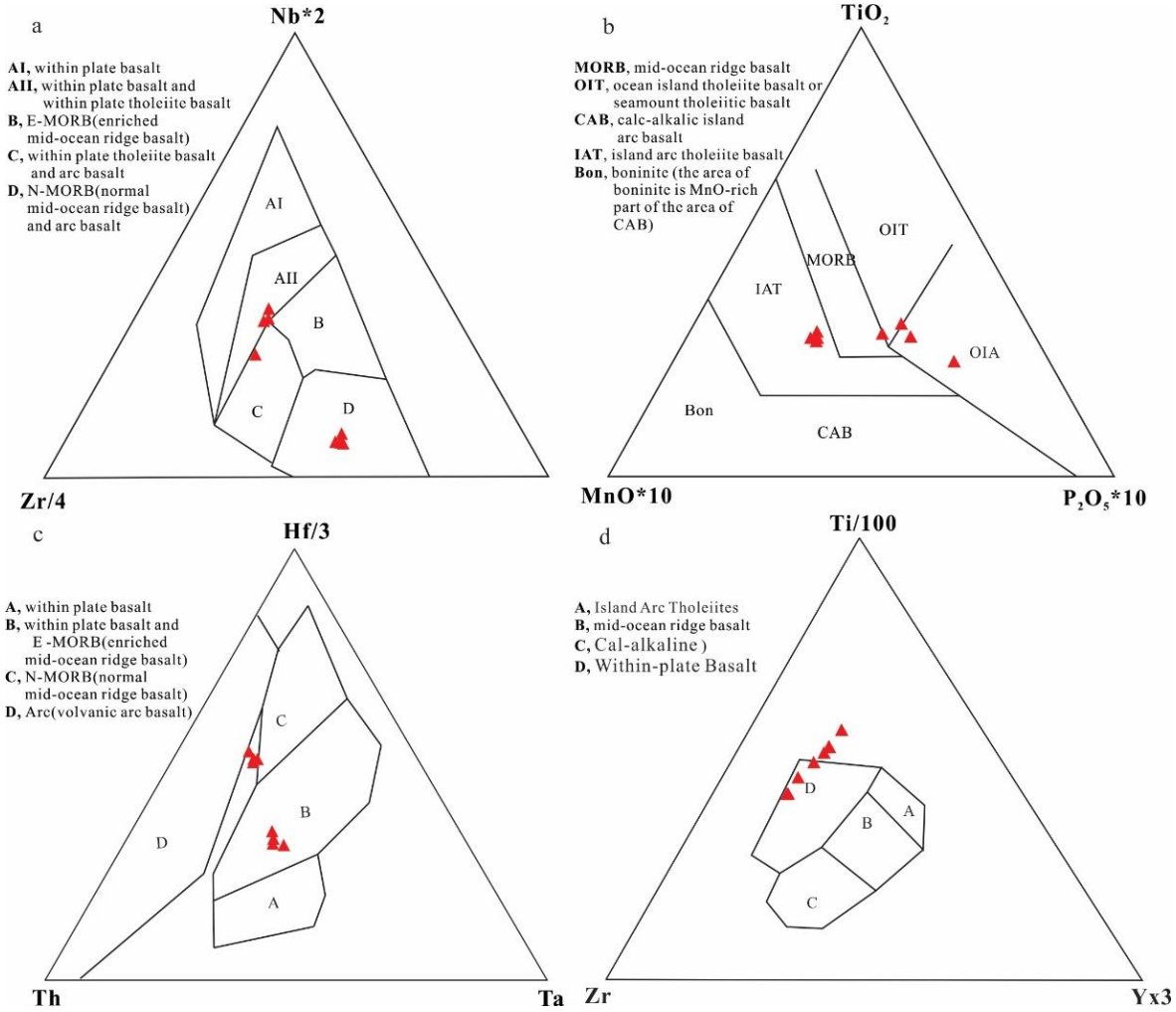

Fig. 11. The discrimination diagrams of (a) Nb*2 – Zr/4-Y of Meschedes. (1986). (b) MnO*10 – P_2O_5*10 – TiO_2 of Mullen. (1983). (c) Hf/3 – Th – Ta of Wood (1980), VAB, MORB and WPB represent Volcanic Arc Basalt, Mid-Ocean Ridge Basalts and Within-Plate Basalt, respectively. (d) Ti/100-Zr-Y*3 for amphibolites from J. Kordofan in El Obeid area. Symbols are the same as those in Fig. 4.

6.5 Tectonic implications

The Neoproterozoic time is very important for Africa continent evolution, the study area which located within the basement Complex of amphibolite facies. Kordofan area is a part of the Saharan Metacraton and the Arabian-Nubian Shield reworking (Fig 1) (Schandelmeier et al., 1990, 1994; Abdel-Rahman et al., 1990b; Stern, 1994; Ibinoof et al., 2016). Two dominant lithologic units formed the Arabian-Nubian Shield; the first one is Island-arc/back-arc basin and the second unit is the Ophiolite assemblages (Abdelsalam et al., 2002). The reworking of the Saharan Metacraton and the Arabian-Nubian Shield during the Neoproterozoic time dominated by deformation (Vail, 1971; 1972; 1976b; Schandelmeier et al., 1987; 1988; Stern, 1994; Abdelsalam and Stern, 1996a, b; Abdelsalam et al., 1998; 2002); metamorphism (Kröner et al., 1987a,b; Stern and Dawoud, 1991); and igneous bodies emplacement (Stern, 1994). Furthermore, restricted oceanic basins had been formed through extension of this continental crust, which later closed due to the collision between the drifted blocks. Kordofan area is one of most exposures of the Saharan Metacraton in Sudan with some Arabian-Nubian Shield rocks (El Khidir, 1996; Abdelsalam et al., 2002; Mustafa, 2007; Eivok, 2013; Ibnoof et al., 2016). During the Neoproterozoic many cratons and belts are formed e.g. the Arabian-Nubian Shield formation, reworking of the eastern margin of East Saharan Craton, formation of the Mozambique Belt in Central and South Africa and Orogen of East African. The orogeny of East African initiated with breakup of Rodinia at ~900-850 Ma coevally with starting of assemblage Gondwanaland. During this collision the juvenile crustal materials with abundant ophiolites in the Arabian-Nubian Shield formed in arc settings (Stern, 1994; El Khidir (1997; Mustafa, 2007). The opening and closing of Red Sea generated the ophiolite of Jebel Rahib and low-grade sedimentary belt in Kordofan in central Sudan, these rock sequences in the Neoproterozoic intruded by granitoid rocks (Abdel Salam et al. 2002). The sequence evolution of the Red Sea Hills sector of the Nubian Shield divided into three periods;

the early period (1200-1000 Ma); the Middle period (1000-600 Ma) and Late Pan African period (600-500 Ma) (Abdel-Rahman, 1993), comparable with the events that supporting ophiolite-arc collision accretion model (Gass, 1981; Abdel-Rahman, 1993;).

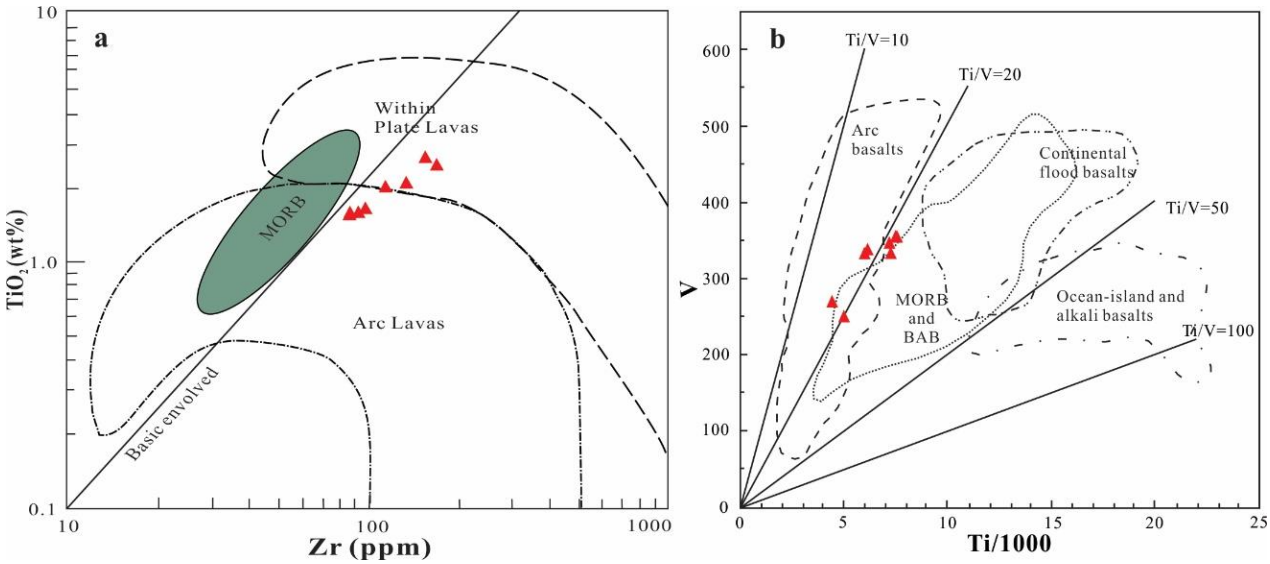

Fig. 12. The discrimination diagrams of TiO_2 vs Zr of Pearce and Cann (1973) and V vs Ti/1000 of Shervais (1982) for amphibolites from J. Kordofan in El Obeid area. Symbols are the same as those in Fig. 4.

Four models had been proposed from Saharan Metacraton remobilization; the first model is collision; The second is delamination of the sub-continental mantle lithosphere; The third is extension; The fourth is metacraton assemblge from exotic terrenes (Abdelsalam et al. 2002). Bayuda area in northern part of Sudan one of the eastern extension of Saharan Metacraton where collided with the Arabian-Nubian Shield along Keraf Zone (Abdelsalam and Stern, 1996b;). The island-arc/back-arc marginal settings and low-grade volcano-sedimentary rocks within the medium to high-grade gneissic terranes of the Arabian-Nubian Shield put this region as a result of accretion on the eastern margin of the Saharan Metacraton (Küster and Liégeois, 2001; Evuk, 2013). The boundary between the Metacraton and the Arabian-Nubian Shield in Sudan goes along Zalingei Fold Zone or further west (Küster and Liégeois, 2001), including Kordofan area where these amphibolites cropped out. Nevertheless, the suture zones in the north and northeast Sudan are originated due to the island-arc/back-arc basin complexes and plate margin type volcano-sedimentary rocks which are in a tectonic contact with the ophiolitic rocks in the region (Kroner, 1985; Ries et al., 1985; Stern et al., 1989, 1994; Harms et al., 1994; Schandelmeier et al., 1994;). The Kordofan region has no relief suture zones although it is a part of overall processes in the Sudan.

The amphibolites from J. Kordofan are located within the basement of Kordofan region which formed coevally with Rodinia supercontinent assemblage. Moreover, these rocks have high-iron content, characterized by significant spiky patterns and arc-like primitive mantle-normalized incompatible-element patterns, and are calc-alkaline to tholeiitic basalts equivalent with amphibolites from J. El Eiza'a and Bayuda area (Evuk, 2013) indicating basaltic volcanism of primitive to more mature oceanic convergent margin of oceanic island arc and/or back-arc setting (Küster and Liegeois, 2001). These amphibolites rocks were derived from a complex mantle source with components having a mildly depleted mantle nature suggesting arc and back arc environment signature for their precursor magma. Finally, we proposed that these rocks intruded during the Neoproterozoic time which dominated by magmatism and metamorphism.

7. Conclusions

Amphibolite rocks from of Jebel Kordofan in North Kordofan State in western Sudan occurred within the Precambrian rocks intruded during the Neoproterozoic. The precursor magmas of these amphibolites were derived from sub-alkali to tholeiite basaltic magmas which derived from metasomatic sub-continental lithospheric mantle melt-related enrichment in arc and back arc tectonic settings environments. The geochemical investigations of these amphibolites linked with the few available data and geological observations in the region and adjacent areas proposed that they were origin during the Saharan Metacraton and the Arabian Nubian Shield reworking through collision-accretion-subduction, possibly coevally with the assemblage of Rodinia Supercontinent during the Neoproterozoic period.

Acknowledgments

The authors acknowledge with gratitude to Professors Chen Nengsong, Ma and Dr. Wang Liangxun for financial support.

References

Abdalla, O.A.E. 1999. Ground Water Hydrology of the West-Central Sudan, Hydrochemical and Isotopic Investigations Flow Similuuation and Resources Management, Verlag Dr. Koster Berlin.

Abdel Mageed, A. 1998. Sudan Industrial Minerals and Rocks, Center for Strategic Studies, Khartoum, Sudan.

Abdel Rahman, E.M., 1993. Geochemical and geotectonic controls of the metallogenic evolution of selected ophiolite complexes from the Sudan. Berl. Geowiss. Abh., A 145 (175 pp).

Abdel Rahman, E.M., Harms, U., Schandelmeier, H., Franz, G., Darbyshire, D.P.F., Horn, P., and Muller-Sohnius. 1990. A new ophiolite occurrence in NW Sudan – constraint on Late Proterozoic Tectonism-Terra Nova, Melbourne-Oxford- London-Paris.2, 363-376.

Abdelsalam, M. G., Liégeois, J. P., and Stern, R. J. 2002. The Saharan Metacraton: Journal of African Earth Sciences, 34, 119–136.

Abdelsalam, M. G., Stern, R.J 1996a. Deformational history of the Neoproterozoic Keraf Zone in NE Sudan revealed by Shuttle Imaging Radar. Journal of Geology, 103, 475-491.

Abdelsalam, M.G. and Stern, R.J. 1996b. Mapping Precambrian structures in the Sahara Desert with SIR-C/X-SAR radar: The Neoproterozoic Keraf Suture, NE Sudan. Journal of Geophysical Research. 101(10), 065-076.

Abdelsalam, M.G., Stern, R.J., Copeland, P., Elfaki, E., Elhur, B., Ibrahim, F.M. (1998). The Neoproterozoic Keraf suture in NE Sudan: sinistral transpression along the eastern margin of west Gondwana. J. Geol., 106, 2: 133-148.

Abdelsalam, M.G., Dawoud, A.S., 1991. The Kabus ophiolitic melange, Sudan, and its bearing on the W boundary of the Nubian Shield. J. Geol. Soc. London 148, 83–92.

Ahijado, A., Casillas, R., Hernandez-Pacheco, A., 2001. The dyke swarms of the Amanay Massif, Fuerteventura, Canary Islands (Spain). Journal of Asian Earth Sciences 19, 333–345.

Ahmed-Said, Y. and Leake, B.E., 1997. The petrogenesis of the Edough amphibolites, Annaba, NE Algeria: two unrelated basic magmas and the lherzolite-harzburgite residue of a possible magma source. Mineralogy and Petrology 59, 207–237.

Al Biely, A., I., Farwa, A. G. and Gism ElSid, N. E. 1986. A Geological, Geophysical and Hydrogeological Investigation In North Kordofan, Department of Geology, University of Khartoum, Khartoum, Sudan.

Belousova, E.A., Griffin, W.L., O'Reilly, S.Y., Fisher, N.I., 2002. Igneous zircon: Trace element compositionas indicator of source rock type. Contributions to Mineralogy and Petrology, 143, 602–622.

Bogdanova, S.V., Pisarevsky, S.A., Li, Z.X., 2009. Assembly and Breakup of Rodinia (Some results of IGCP project 440). Stratigraphy and Geological Correlation. 17 (3) 29 – 45.

Burg, J.P., 2011. The Asia–Kohistan–India collision: review and discussion. In: Arc-Continent Collision. Springer, Berlin, Heidelberg, pp. 279–309.

Cai, K. D., Sun, M., Xiao, W. J., et al. 2014. Petrogenesis of late Paleozoic tholeiitic, Nb-enriched, calc-alkaline and adakitic rocks in southwestern Mongolia: Implications for intra-oceanic arc evolution. Lithos, 202–203, 413–428.

Castro, A., Vogt, K., Gerya, T., 2013. Generation of new continental crust by sublithospheric silicic-magma relamination in arcs: a test of Taylor's andesite model. Gondwana Res. 23 (4), 1554–1566.

Collins, A. S. 2003. Structure and Age of the Northern Leeu- win Complex, Western Australia: Constraints from Field Mapping and U–Pb Isotopic Analysis," Australian Journal of Earth Science. 50, 585–599.

Condie, K. C., Viljoen, M.J., Kable, E.J.D., 1977. "Effects of alteration on element distributions in Archean tholeiites from the Barberton greenstone belt, South Africa." Contributions to Mineralogy and Petrology 64, 75-89.

Condie, K.C., 1997. Sources of Proterozoic mafic dyke swarms: constraints from Th/Ta and La/Yb ratios. Precambrian Research 81, 3–14.

Corfu, F., Hanchar, J.M., Hoskin, P.W.O., Kinny, P., 2003. Atlas of Zircon Textures. Mineralogy and Geochemistry, 53(1), 469-500.

Cullers, R.L., Yeh, L.T., Choudhuri, S., Guidotti, C.V., 1974. Rare earth elements in Silurian schists from N.W. Maine. Geochemistry Geosystems Acta 38, 389-400.

DeBari, S.M., Greene, A.R., 2011. Vertical stratification of composition, density, and inferred magmatic processes in exposed arc crustal sections. In: Arc-Continent Collision. Springer, Berlin, Heidelberg, pp. 121–144.

Defant, M. J., Jackson, T. E., Drummond, M. S. 1992. The geochemistry of young volcanism throughout western Panama and southeastern Costa Rica: An overview. Journal of the Geological Society of London, 149, 569–579.

Elageed, A.I and Elrabaa, S.M.E., 1981. The Geology and Structural Evolution of the Northeastern Nuba Mountain Kordofan Province, Sudan, Bulletin No 32, Ministry of Energy and Mining Geology and Mineral Resources Department, Sudan.

ElKhidir, S.O.H. (1997): Metamorphic Evolution of Sodari-Umm Badr Area –North Kordofan, Sudan. (unpublished M.Sc. Thesis) University of Khartoum.

Ernst, R.E., Bleeker, W., Söderlund, U., Kerr, A.C., 2013. Large Igneous Provinces and supercontinents: Toward completing the plate tectonic revolution, Lithos 174, 1–14.

Ernst, R.E., Wingate, M.T.D., Buchan, K.L., Li, Z.X., 2008. Global record of 1600–700 Ma Large Igneous Provinces (LIPs): implications for the reconstruction of the proposed Nuna (Columbia) and Rodinia supercontinents. Precambrian Research 160,159–178.

Ernst, R.E., Buchan, K.L., 2001. Large mafic magmatic events through time and links to mantle plume heads. In: Ernst, R.E., Buchan, K.L. (Eds.), Mantle Plumes: Their Identification through Time. Special Paper Geological Society of America 352, 483–575.

Ernst, R.E., Buchan, K.L., 1997. Giant radiating dyke swarms: their use in identifying pre-Mesozoic large igneous provinces and mantle plumes. In: Mahoney, J.J., Coffin, M.E. (Eds.), Large Igneous Provinces: Continental, Oceanic, and Planetary Flood Volcanism. Geophysical Monograph, vol. 100, pp. 297–333.

Evuk, D. O. O., 2013. Geodynamic evolution of the central-eastern Bayuda Desert Basement, Sudan: Structural, petrological, geochemical and geochronological investigations. Ph.D Thesis Technischen University, Berlin.

Fan, W.-M., Guo, F., Wang, Y.-J., Zhang, M., 2004. Late Mesozoic volcanism in the northern Huaiyang tectono-magmatic belt, central China: partial melts from a lithospheric mantle with subducted continental crust relicts beneath the Dabie orogen? Chemical Geology 209, 27–48.

Fenner, C.N., 1929. The crystallization of basalt. American Journal of Science 18, 223–253.

Foster, B.D.F. 1994. Origin and Tectonic Significance of Peninsular Ranges Amphibolites, Ph.D. thesis Faculty of San Diego State University (unpublished).

Francalanci, L., Tommasini, S., Conticelli, S., Davies, G. R., 1999. Sr isotope evidence for short magma residence time for the 20th century activity at Stromboli volcano. Italy. Earth and Planetary Science Letters 167, 61 – 69.

Frimmel, H. E., Zartman, R.E., Spath, A. 2001. The Rich- tersveld Igneous Complex, South Africa: U–Pb Zircon and Geochemical Evidence for the Beginning of Neoproterozoic Continental Breakup, Journal of Geology 109, 493–508.

Garrido, C.J., Bodinier, J.L., Dhuime, B., Bosch, D., Chanefo, I., Bruguier, O., Hussain, S.S., Dawood, H., Burg, J.P., 2007. Origin of the island arc Moho transition zone via melt-rock reaction and its implications for intracrustal differentiation of island arcs: evidence from the Jijal complex (Kohistan complex, northern Pakistan). Geology 35 (8), 683–686.

Gass, I.G. 1981. Pan-African (Late-Proterozoic) plate tectonics of Arabian-Nubian Shield. In: Precambrian plate tectonics (edited by Kroner, A.), Amsterdam, 357-405.

Gazel, E., Hayes, J.L., Hoernle, K., Kelemen, P., Everson, E., Holbrook, W.S., Hauff, F., van den Bogaard, P., Vance, E.A., Chu, S., Calvert, A.J., Carr, M.J., Yogodzinski, G.M., 2015. Continental crust generated in oceanic arcs. Nat. Geosci. 8 (4),321–327.

Gebauer, D.A., 1996. P-T-t path for an (ultra-?) high pressure ultramafic-mafic rock association and its felsic country rocks based on SHRIMP—— dating of magmatic and metamorphic zircon domains. Example: Alpe Arami (Central Swiss Alps). In: Earth Processes Reading the Isotopic Code, Geophysical Monograph 95, 307–329.

Geringer, G.J., 1979. The origin and tectonic setting of amphibolites in part of Namaqua Metamorphic Belt, South Africa, Traa'. Geological Society South Africa 82, 287–303.

Goldberg, A.S., 2010. Dyke swarms as indicators of major extensional events in the 1.9–1.2 Ga Columbia supercontinent. Journal of Geodynamics 50, 176–190.

Harms, U., Darbyshire, D.P.F., Denkler, T., Hengst, M. and Schandelmeier, H. 1994. Evolution of the Neoproterozoic Delgo Suture Zone and crustal growth in northern Sudan: geochemical and radiogenic isotope constrains. Geologische Rundsch. 83, 591–603.

Harms, U., Schandelmeier, H., Darbyshire, D.P.F., 1990. Pan-African reworked early/ middle Proterozoic crust in NE Africa W of the Nile: Sr and Nd isotope evidence. J. Geol. Soc. London 147, 859–872.

Hidaka, H, Shimizu, H, Adachi, M, 2002. U-Pb geochronology and REE geochemistry of zircons from Palaeoproterozoic paragneiss clasts in the Mesozoic Kamiaso conglomerate, central Japan: Evidence for an Archean provenance. Chemical Geology 187, 278–293.

Hofmann, A.W., Jochum, K.P., 1996. Source characteristics derived from very incompatible trace elements in Mauna Loa and Mauna Kea basalts, Hawaii Scientific Drilling Project. J. Geophys. Res. 101 (B5), 11831–11839.

Hollings, P., Kerrich, R. 2004. Geochemical systematics of tholeiites from the 2.86 Ga Pickle Crow Assemblage, northwestern Ontario: arc basalts with positive and negative Nb-Hf anomalies. Precambrian Research, 134, 1–20.

Hoskin, P.W.O., Ireland, T.R., 2000. Rare earth element chemistry of zircon and its use as a provenance indicator. Geology 28(7), 627–630.

Hou, G.T., 2012. Mechanism for three types of mafic dyke swarms. Geoscience Frontiers 3(2), 217–223.

Ibinoof, M. A., Bumby, A. J., Grantham, G. H., Abdelrahman, E. M., Eriksson, P. G., le Roux, P. J. 2016. Geology, geochemistry and Sr–Nd constraints of selected metavolcanic rocks from the eastern boundary of the Saharan Metacraton, southern Sudan: A possible revision of the eastern boundary. Precambrian Research, 281, 566–584.

Irvine, T.N., Baragar, W.R.A., 1971. A guide to the chemical classification of the common volcanic rocks Can Journal Earth Sciences 8, 523–548.

Kamber, B.S. 2015. The evolving nature of terrestrial crust from the Hadean, through the Archaean, into the Proterozoic Precambrian

Research 258, 48–82

Kelley, K.A., Plank, T., Ludden, J., Staudigel, H., 2003. Composition of altered oceanic crust at ODP Sites 801 and 1149. Geochemistry Geophysics Geosystem 4.

Kepezhinskas, P., McDermott, F., Defant, M.J., Hochstaedter, A., Drummond, M.S., 1997. Trace element and Sr–Nd–Pb isotopic constraints on a three-component model of Kamchatka Arc petrogenesis. Geochim. Cosmochim. Acta 61 (3), 577–600.

Kröner, A. 1985. Ophiolites and evolution of tectonic boundaries in the Late-Proterozoic Arabian-Nubian Shield of NE Africa and Arabia. Precambrian Res., vol. 27, 277-300.

Kröner, A., Greilling, R., Reischmann, T., Hussein, I.M., Stern, R.J., Dürr, S., Kruger, J., and Zimmer, M., 1987a. Pan-African crustal evolution in the Nubian segment of the NE Africa, in Kröner, A., (ed.), Proterozoic lithospheric evolution: Am. Geophys. Union Geodynamics series 17, 235-257.

Kröner, A., Stern, R.J., Dawoud, A.S., Compston, W., Reischmann, T. 1987 b. The Pan- African continental margin in NE Africa: evidence from the geochronological study of granulites at Sabaloka, Sudan. Earth Planetary Science Letters 85, 91-104.

Küster, D., Liégeois, J.P., Matukov, D., Sergeev, S., Lucassen, F., 2008. Zircon geochronology and Sr, Nd, Pb isotope geochemistry of granitoids from Bayuda Desert and Sabaloka (Sudan): evidence for a Bayudian event (920–900 Ma) preceding the Pan-African orogenic cycle (860–590 Ma) at the eastern boundary of the Saharan Metacrat. Precambrian Research. 164, 16–39.

Küster, D., Liégeois, J. P. 2001. Sr, Nd isotopes and geochemistry of the Bayuda Desert high-grade metamorphic-basement (Sudan): an early Pan-African oceanic convergent margin, not the edge of the East Saharan ghost craton. Precambrian Research, 109, 1-23.

LaFle`che, M.R., Camire′, G., Jenner, G.A., 1998. Geochemistry of post-Acadian, Carboniferous continental intraplate basalts from the Maritimes basin, Magdalen islands, Que′bec, Canada. Chemical Geology 148, 115–136.

Leat, P.T., Larter, R.D., 2003. Intra-oceanic subduction systems: introduction. In: Larter, R.D., Leat, P.T. (Eds.), Intra-Oceanic Subduction Systems: Tectonic and Magmatic Processes, vol. 219. Geological Society, London, pp. 1–17, Special Publications.

Lebas, M.J., Lemaitre, R.W., Streckeisen, A. and Zanettin, B. 1986. A Chemical Classification of Volcanic-Rocks Based on the Total Alkali Silica Diagram. Journal of Petrology 27(3): 745-750.

Li, Z. X., Li, X.H., Kinny, P.D., Wang, J. 1999. The Breakup of Rodinia: Did it Start with a Mantle Plume Beneath South China?. Earth Planetary Science Letters. 173 (3), 171–181.

Liu, Y.S., Hu, Z.C., Zong, K.Q., Gao, C.G., Gao, S., Xu, J., Chen, H.H., 2010. Reappraisement and refinement of zircon U-Pb isotope and trace element analyses by LA-ICP-MS. Chinese Science Bulletin, 55(15): 1535–1546.

Liu, Y.S., Hu, Z.C., Gao, S., Günther, D., Xu, J., Gao, C.G., Chen, H.H., 2008. In situ analysis of major and trace elements of anhydrous minerals by LA-ICP-MS without applying an internal standard. Chemical Geology 257, 34–43.

Lu, S.N., Li, H.K., Zhang, C.L., Niu, G.H., 2008. Geological and Geochronological evidences for the Precambrian evolution of the Tarim Craton and surrounding continental fragments. Precambrian Research 160, 94–107.

Ludwig, K.R., 2003. ISOPLOT 3.00: A Geochronological Toolkit for Microsoft Excel (Berkeley Geochronology Center, Berkeley, California). BGC Special Publ. 1a, Berkeley, 55 pp.

Mayborn, K.R., Lesher, C.E., 2004. Paleoproterozoic mafic dike swarms of northeast Laurentia: products of plumes or ambient mantle?. Earth and Planetary Science Letters 225, 305–317.

Mazhari, S. A. 2016. Petrogenesis of adakite and high-Nb basalt association in the SW of Sabzevar Zone, NE of Iran: Evidence for slab meltemantle interaction. Journal of African Earth Sciences, 116, 170–181.

McBirney, A. R. and H. Naslund (1990). "The differentiation of the Skaergaard intrusion." Contributions to Mineralogy and Petrology 104(2), 235-240.

Mcculloch, M.T., Gamble, J.A., 1991. Geochemical and geodynamical constraints on subduction zone magmatism. Earth and Planetary Science Letters 102, 358–374.

Meert J. G. and Van der Voo, R. 1997. The Assembly of Gondwana 800–550 Ma, Journal of Geodynamics 23, 223–236.

Meschede, M. (1986). A method of discriminating between different types of mid-ocean ridge basalts and continental tholeiites with the Nb-Zr-Y diagram.

Miyashiro, A., Shido, F., 1975. Tholeiitic and calc-alkalic series in relation to the behaviors of titanium, vanadium, chromium and nickel. American Journal of Science 275, 265-277.

Moller, A., O'Brien, P.J., Kennedy, A., Kennedy, A., Krone, A., 2003. Linking growth episodes of zircon and metamorphic textures to zircon chemistry: An example from the ultrahigh-temperature granulites of Rogaland (SW Norway). EMU Notes in Mineralogy, 5,65–82.

Mullen E.D., 1983. $MnO/TiO_2/P_2O_5$: a minor element discriminant for basaltic rocks of oceanic environments and its implications for petrogenesis. Earth and Planetary Science Letters 62, 53–62.

Mustafa, H. A., 2007. A concept of the relationship between metamorphism and structures in El Obeid area North Kordofan State Sudan. M.Sc. Thesis, University of Kordofan.

Pearce, J.A., 1996. A user's guide to basalt discrimination diagrams. In: Wyman, D.A. (ed.), Trace Element Geochemistry of Volcanic Rocks: Applications for Massive Sulfide Exploration. Geological Association of Canada, Short Course Notes. 12, 79–113.

Pearce, J.A., 1982. Trace Element characteristics of the lava from destructive plate boundaries in Andesites (R.S. Thorpe ed.) pp. 525-547.

Pearce, J.A., Nigel, B. W., Harris and Andrew, G. Trindle. 1984. Trace Element Discrimination Diagrams for the Tectonic Interpretation of Granitic Rocks. Department of Earth Sciences, The Open University, Milton Keynes, MK76AA, Bucks, England.

Pearce, J.A., Norry, M.J. 1979. Petrogenetic implications of Ti, Zr, Yand Nb variations in volcanic rocks. Contribution of Mineral Petrology 69, 33-47.

Pearce, J.A., Cann, J.R., 1973. Tectonic setting of basic volcanic rocks determined using trace element analyses. Earth and Planetary Science Letters 19, 290–300.

Peng, P., Zhai, M.G., Guo, J.H., Kusky, T., Zhao, T.P., 2007. Nature of mantle source contributions and crystal differentiation in the petrogenesis of the 1.78 Ga maf ic dykes in the central North China craton. Gondwana Research 12, 29–46.

Petrone, C. M., Ferrari, L. 2008. Quaternary adakite–Nb-enriched basalt association in the western Trans-Mexican Volcanic Belt: is there any slab melt evidence? Contributions to Mineralogy and Petrology, 156, 73–86.

Pisarevsky, S. A., Wingate, M. T. D., Powell, C, M., 2008. Models of Rodinia assemblage and Fragmentation. In Yoshida, M., Windley, B. F., Dasgupta, S. (eds) Proterozoic East Gondowana Supercontinent assembly and breakup. Geological Society. Special publications. 206, 35- 55.

Pisarevsky, S. A. 2005. New Edition of the Global Paleomagnetic Database. EOS Trans. American Geophysics Union. 86 (17), 170.

Radhakrishna T. and Mathew, J. 1996. Late Precambrian (850–800 Ma) Palaeomagnetic Pole for the South Indian Shield from the Harohalli Alkaline Dykes: Geotectonic Implications for Gondwana Reconstructions," Precambrian Research. 80, 77–87.

Ries, A.C., Shackleton, R.M., Dawoud, A.S. 1985. Geochronology, geochemistry and tectonics of the NE Bayuda Desert in northern Sudan: Implication for the western margin of the late Proterozoic fold belt of NE Africa. Precambrian Research 30, 43-62.

Rollinson, H.R., 1993. Using geochemical data: Evaluation, Presentation, Interpretation. Longman, New York, 352pp.

Rodis, H.J, Hassan, A and Wahadan, L. 1964. Ground Water Geology of Kordofan Province Bulletin No. 14, Ministry of Mineral Resources, Geological Survey Department, Khartoum, Sudan.

Rubatto, D., 2002. Zircon trace element geochemistry: Partitioning with garnet and the link between U Pb ages and metamorphism. Chemical Geology, 184, 123–138.

Rubatto, D., Gebauer, D., 2000. Use of cathodoluminescence for U-Pb zircon dating by IOM Microprobe: Some examples from the western Alps. Cathodoluminescence in Geoscience, Springer-Verlag Berlin Heidelberg, Germany, 373–400.

Rudnick, R.L., Gao, S., 2003. Composition of the continental crust. In Rudnick, R.L. (ed), The Crust. Holland, H.D. and Turekian, K.K. (eds), Treatise on Geochemistry. Elsevier-Pergamon, Oxford 3, 1–64.

Rudnick, R.L., Fountain, D.M., 1995. Nature and composition of the continent-crust: a lower crustal perspective. Rev. Geophys. 33 (3), 267–309.

Rudnick, R.L., 1995. Making continental crust. Nature 378 (6557), 571–577. Rudnick, R.L., Gao, S., 2003. Composition of the continental crust. Treatise Geochem. 3, 1–64.

Sajona, F. G., Maury, R. C., Bellon, H., et al. 1996. High field strength element enrichment of Pliocene–Pleistocene island arc basalts, Zamboanga Peninsula, western Mindanao Philippines. Journal of Petrology, 37, 693–726.

Shervais, J.W., 1982. Ti–V plots and the petrogenesis of modern and ophiolitic lavas. Earth and Planetary Science Letters 59, 101–118.

Schandelmeier, H., Darbyshire, D.P.F., Harms, U., Richter, A. 1988. The E Saharan Craton: evidence for pre-Pan-African crust in NE Africa W of the Nile. In: El Gaby, S., Greiling, R.O. (Eds.). The Pan-Africa belts in NE Africa and Adjacent areas. Friedr. Vieweg and Sohn.. 69-94.

Schandelmeier, H., Richter, A., Harms, U. 1987. Proterozoic deformation of the East Saharan Craton in southeast Libya, South Egypt and North Sudan. Tectono Physics 140, 233-246.

Schandelmeier, H., Richter, A., Harms, U., Abdel Rahman, E.M. 1990. Lithology and structure of the late Proterozoic Jebel Rahib fold-and-thrust belt (SW Sudan). Berliner Geowissen Abher (A) 120. 1, 15-30.

Schandelmeier, H., Wipfler, E., Küster, D., Sultan, M., Becker, R., Stern, R.J., Abdelsalam, M.G. 1994. Atmur Delgo suture: A Neoproterozoic oceanic basin extending into the interior of northeast Africa. Geology 22, 563-566.

Sklyarov, E.V., Gladkochub, D.P., Mazukabzov, A.M., Menshagin, Y.V., Watanabe, T., Pisarevsky, S.A., 2003. Neoproterozoic mafic dike swarms of the Sharyzhalgai metamorphic massif, southern Siberian craton. Precambrian Research 122, 359–376.

Sobolev, A.V., Hofmann, A.W., Nikogosian, I.K., 2000. Recycled oceanic crust observed in 'ghost plagioclase' within the source of Mauna Loa Lavas. Nature 404, 986–990.

Staudigel, H., Davies, G.R., Hart, S.R., Marchant, K.M., Smith, B.M., 1995. Large scale isotopic Sr, Nd and O isotopic anatomy of altered oceanic crust: DSDP/ODP sites 417/ 418. Earth and Planetary Science Letters 130, 169–185.

Stein M. and Goldstein, S. L. 1996. From Plume Head to Continental Lithosphere in the Arabian–Nubian Shield," Nature 382, 773–778.

Stein, M. and Hofmann, A.W. 1994. Mantle plumes and episodic crustal growth. Nature 372, 63-68.

Stern, R.J., 2010. The anatomy and ontogeny of modern intra-oceanic arc systems. Geol. Soc. London 338 (1), 7–34, Special Publications.

Stern, R.J. 1994. Arc assembly and continental collision in the Neoproterozoic East African Orogen; implication for the

consolidation of Gondwanaland. Annual Reviews of Earth and Planetary Science 22, 319-351.

Stern, R.J. and Dawoud, A.S. 1991. Late Precambrian (740Ma) Charnokite, Enderbite, and granite from Jebel Moya, Sudan: a link between the Mozambique Belt and the Arabian- Nubian Shield? Journal of Geology. 99, 648-659.

Stern, R.J., Kröner, A., Manton, W.I., Reischmann, T., Mansour, M., Hussein, I.M. 1989. Geochronology of the late Precambrian Hamisana shear zone, Red Sea Hills, Sudan and Egypt. Journal of Geological Society, London, 146, 1017-1029.

Sun, S.S., McDonough, W.F., 1989. Chemical and isotopic systematics of oceanic basalt: implications for mantle composition and processes. In Sanders, A.D., Norry, M.J. (eds.), Magmatism in the Ocean Basins. Geological Society. Special Publication, London 42, 313–345.

Tatsumi, Y., Shukuno, H., Tani, K., Takahashi, N., Kodaira, S., Kogiso, T., 2008. Structure and growth of the Izu–Bonin–Mariana arc crust: 2. Role of crust–mantle transformation and the transparent Moho in arc crust evolution. J. Geophys. Res.: Solid Earth (1978–2012) 113, B2.

Taylor, S.R., McLennan, S.M., 1995. The geochemical evolution of the continental crust. Rev. Geophys. 33 (2), 241–265.

Taylor, S.R., McLennan, S.M., 1985. The Continental Crust: Its Composition and Evolution. Blackwell, Oxford Press, pp. 1–312.

Taylor, R. N., Nesbitt, R. W. 1998. Isotopic characteristics of subduction fluids in an intra- oceanic setting, Izu- Bonin Arc, Japan. Earth and Planetary Science Letters, 164, 79–98.

Thompson, R.N., Morrison, M.A., 1988. Asthenospheric and lower-lithospheric mantle contributions to continental extension magmatism: an example from the British Tertiary Province. Chemical Geology 68, 1–15.

Vail, J.R., 1990. Geochronology of the Sudan. Overseas Geology and Mineral Resources, vol. 66.

Vail, J.R. 1978. Outline of the geology and mineral deposits of the Democratic Republic of the Sudan and adjacent areas. Overseas Geol. Miner. Resour., 49, 67 pp., London.

Vail, J.R., 1973. Outline of the Geology of the Nuba Mountains and Vicinity Southern Kordofan Province, Sudan, vol. 23. Bulletin of the Geological and Mineral Resources Authority of the Sudan.

Vail, J.R. 1972. Geological reconnaissance in the Zalingei and Jebel Marra areas of western Darfur Province. Sudan Geological Survey Department Bulletin 14, 50 p.

Vail, J.R., 1971. Geological reconnaissance in part of Berber District, Northern Province, Sudan: Sudan Geol. Survey Dept. Bull. 18, 76.

Wager, L.R., 1960. The major element variation of the layered series of the Skaergaard intrusion and a re-estimation of the average composition of the hidden layered series and of the successive residual magmas. Journal of Petrology 1, 364–398.

Walker, K.B., Joplin, G.A., Lovering, J.F. and Green, R., 1960. Metamorphic and metasomatic convergence of basic igneous rocks and lime-magnesia sediments of the Precambrian of northwestern Queensland. Geological Society of Australia. 6, 149–178.

Wang,Y.J., Zhao, G.C, Cawood, P.A., Fan, W.M., Peng, T.P., Sun, L.H., 2008b. Geochemistry of Paleoproterozoic (1770 Ma) mafic dikes from the Trans-North China Orogen and tectonic implications. Journal of Asian Earth Sciences 33, 61–77.

Wang, Y.J., Zhao, G.C., Fan, W.M., Peng, T.P., Sun, L.H., Xia, X.P., 2007. LA–ICP-MS U–Pbzircon geochronology and geochemistry of Paleoproterozoic mafic dikes from western Shandong Province: implications for back-arc basin magmatism in theEastern North China Craton. Precambrian Research. 154 (1–2), 107–124.

Weil, A. B., Van der Voo R., Niocaill, M. C., Meert, J. G., 1998. The Proterozoic supercontinent Rodinia: paleomagnetically derived reconstructions for 1100 to 800 Ma. Earth and Planetary Science Letters 154, 13–24.

Wingate, M. T. D., Campbell, I.H., Compston, W., Gibson, G. M. 1998 Ion Microprobe U–Pb Ages for Neoproterozoic Basaltic Magmatism in South-Central Australia and Implications for the Breakup of Rodinia. Precambrian Research, 87, 135–159.

Whiteman, A.J., 1971. The Geology o the Sudan Republic, Oxford, England.

Wood, D. A., 1980. The application of a Th-Hf-Ta diagram to problems of tectono- magmatic classification and to establishing the nature of crustal contamination of basaltic lavas of the British Tertiary volcanic province. Earth and Planetary Science Letters 50, 11-30.

Wu, Y.B., Zheng Y.F., 2004. Research of zircon genetic mineralogy and its conatrain to U-Pb age explaination. Chinese Science Bulletin, 49(16), 1589–1604 (in Chinese).

Wu, Y.B., Chen, D.G., Xia, Q.K., Tu, X.L., Cheng, H., 2002. Micro region trace element analysis of the eclogite in Huang town, Dabie Mountain: trace element characteristic of eclogite facies metamorphic zircon. Chinese Science Bulletin 47(11), 859–863 (in Chinese).

Xiao, Y.Y., Niu, Y.L., Song, S.G., Davidson, J., Liu, X.M., 2013. Elemental responses to subduction-zone metamorphism: Constraints from the North Qilian Mountain, NW China. Lithos. 160–161, 55–67.

Xu, Y.G., Mei, H.J., Xu, J.F., Huang, X.L., Wang, Y.J., Chuang, S.L., 2003. Origin of two differentiation trends in the Emeishan flood basalts. Chinese Science Bulletin 48, 390–394.

Zhang, C.L., Li, Z.X., Li, X.H., Ye, H.M., 2009. Neoproterozoic mafic dyke swarms at the northern margin of the Tarim Block. NW China: age, geochemistry, petrogenesis and tectonic implications. Journal of Asian Earth Science 35, 167–179.

Zhang, Z. C., Kang, J. L., Kusky, T., et al. 2012. Geochronology, geochemistry and petrogenesis of Neoproterozoic basalts from Sugetbrak, northwest Tarim block, China: Implications for the

onset of Rodinia supercontinent breakup. Precambrian Research, 220–221, 158–176.

Zhao, J.H., Zhou, M.F., Ping, Z.J., 2010. Metasomatic mantle source and crustal contamination for the formation of the Neoproterozoic mafic dike swarm in the northern Yangtze Block, South China. Lithos 115, 177–189.

Zhao, J.H., Hu, R.Z., Zhou, M.F., Liu, S., 2007. Elemental and Sr–Nd–Pb isotopic geochemistry of Mesozoic mafic intrusions in southern Fujian Province, SE China: implications for lithospheric mantle evolution. Geological Magazine 144, 937–952.

Zhao, J.H., Zhou, M.F., 2009. Secular evolution of the Neoproterozoic lithospheric mantle underneath the northern margin of the Yangtze Block, South China. Lithos 107, 152–168.

Zhao, G. C., Sun, M., Wilde, S. A., 2002. Reconstruction of a pre-Rodinia supercontinent: New advances and perspectives. Chinese Science Bulletin, 47 (19), 1585–1588.

Zhao, Z.H., 2010. Banded iron formation and related great oxidation event. Earth Science Frontiers 17, 1–12 (in Chinese with English abstract).

Zhou, J., Li, X. H., Ge, W. C., et al. 2007. Age and origin of middle Neoproterozoic mafic magmatism in southern Yangtze Block and relevance to the break-up of Rodinia. Gondwana Research, 12,184 –197.

Zou, H.B., Zindler, A., Xu, X.S., Qi, Q., 2000. Major, trace element, and Nd, Sr and Pb isotope studies of Cenozoic basalts in SE China: mantle sources, regional variations, and tectonic significance. Chemical Geology 171, 33–47.